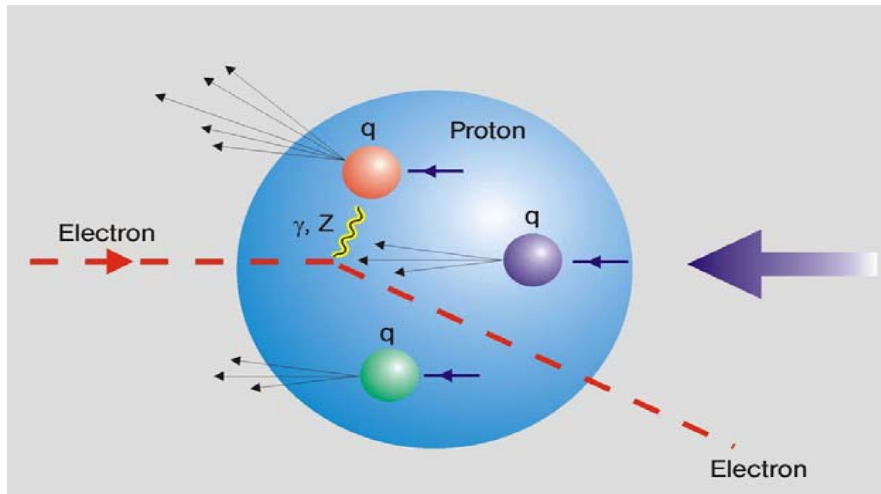


Study of DIS inclusive and diffractive scattering with the ZEUS forward plug calorimeter

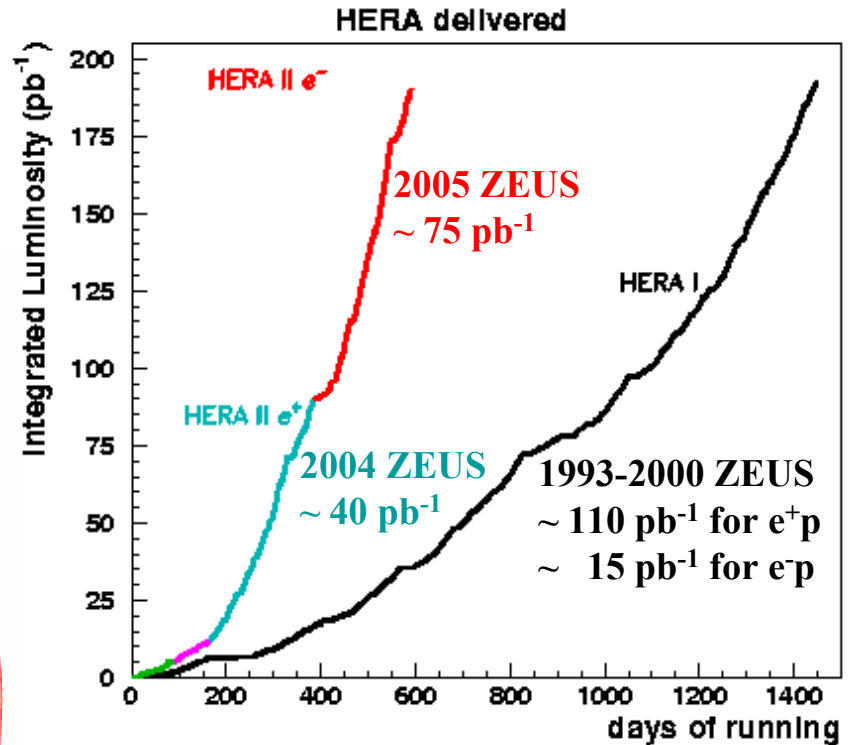
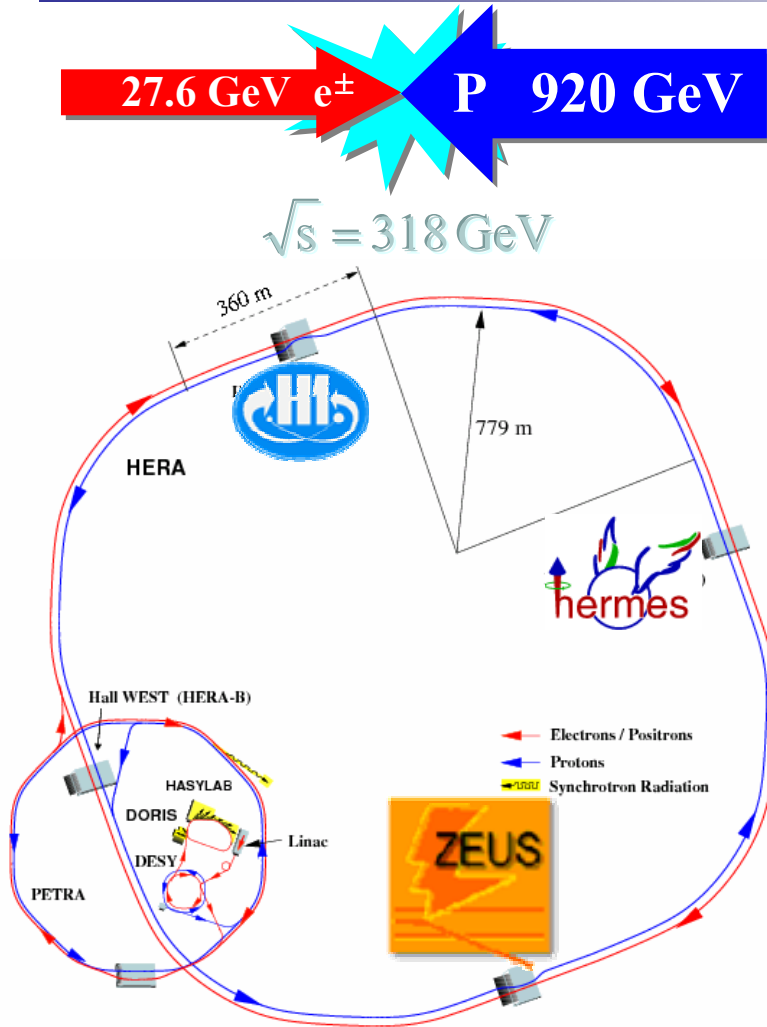
Fermilab, Batavia, Illinois, U.S.A., July 19, 2005

Heuijin Lim (DESY)



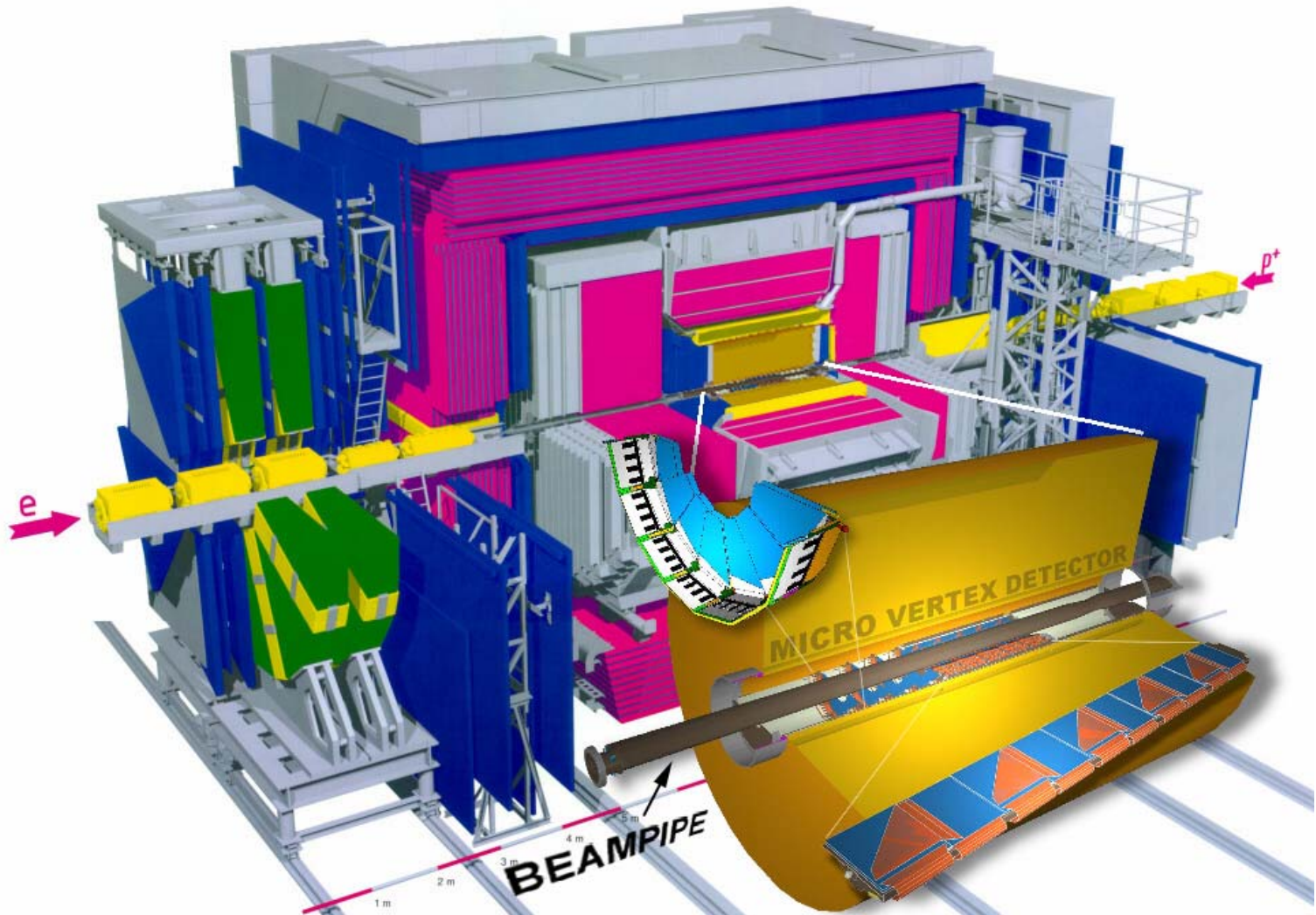
- Introduction
- HERA and ZEUS detector
- Forward plug calorimeter
- Diffractive measurement
- Phenomenology of F_2
- Summary

HERA ep Collider at DESY

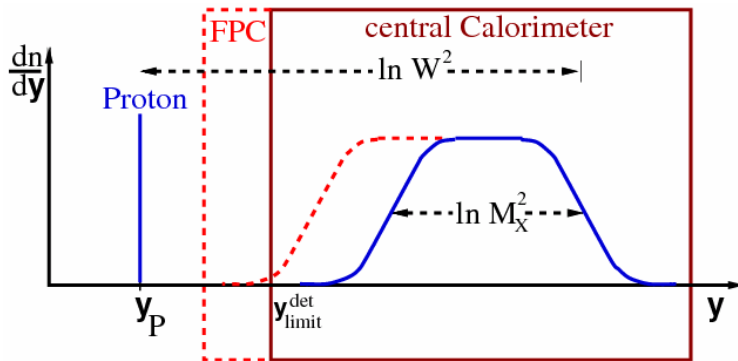
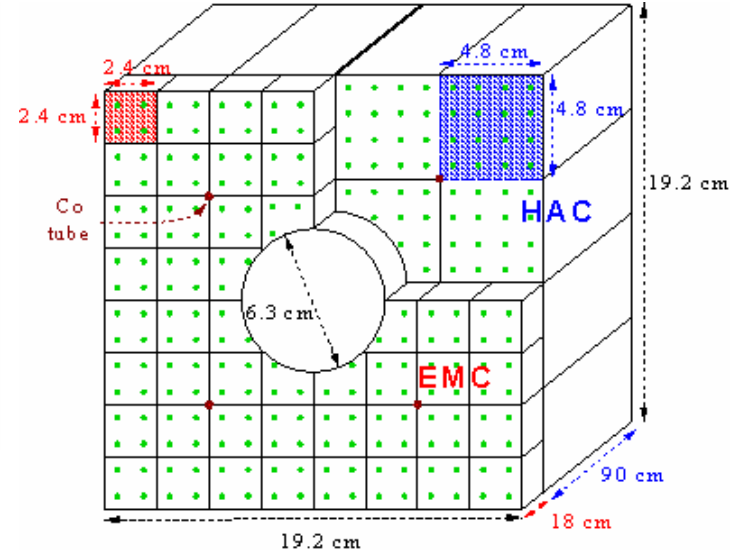
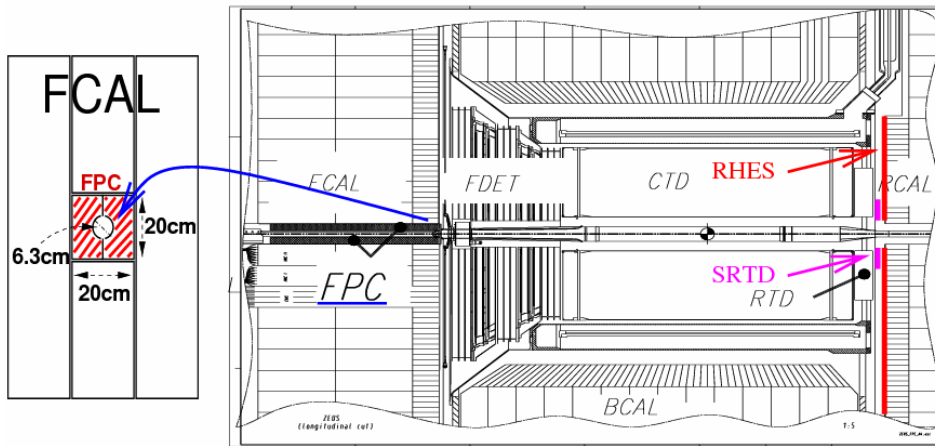


- **ZEUS and H1** : Colliding beam experiments
- **HERMES** : Use the longitudinally polarized e^\pm beams on the polarized gas jet target for the study of the spin structure of the nucleon.

ZEUS Detector



Forward Plug Calorimeter



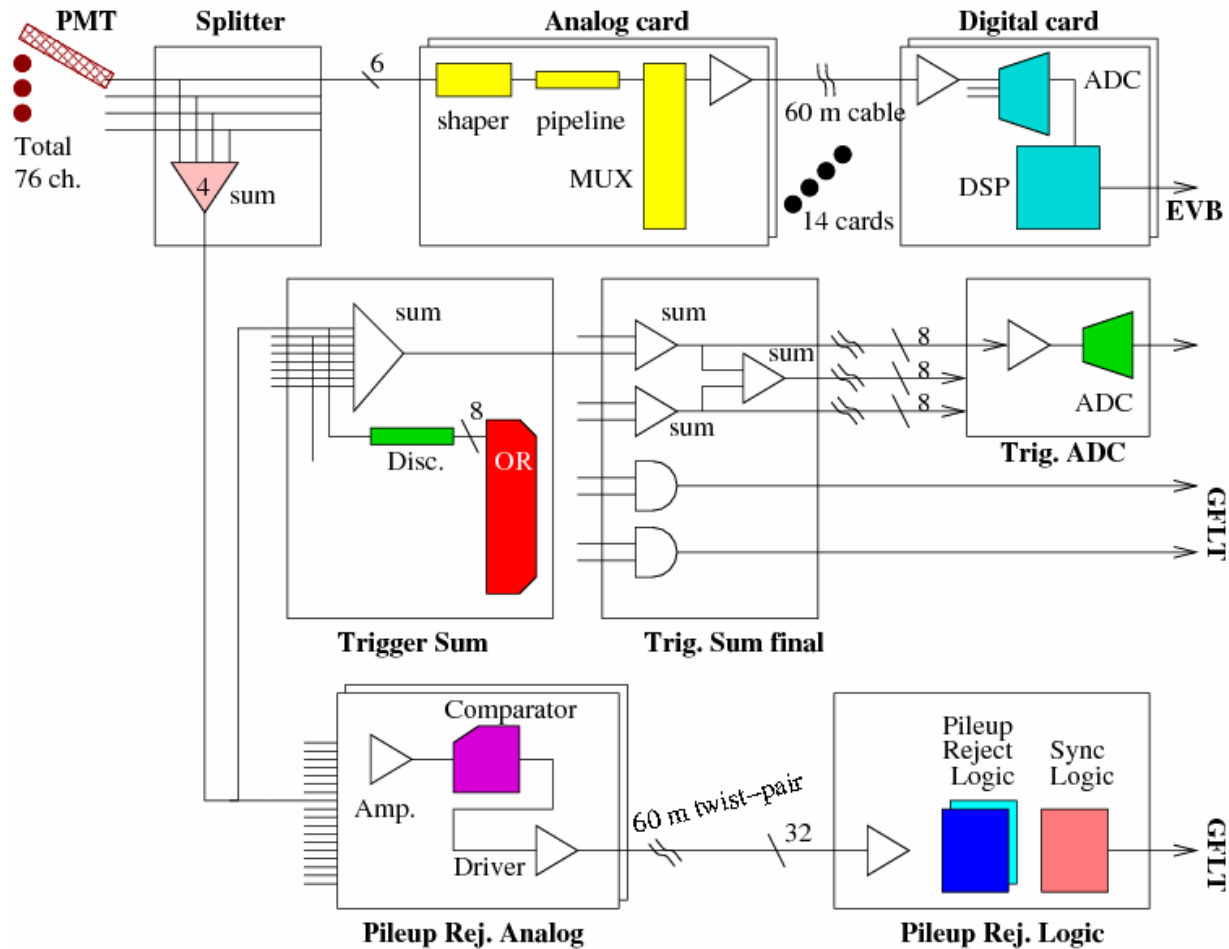
$$\text{rapidity : } \mathcal{Y} = \frac{1}{2} \ln \frac{E + pZ}{E - pZ}$$

$$\text{pseudo-rapidity : } \eta = -\ln \tan\left(\frac{\theta}{2}\right)$$

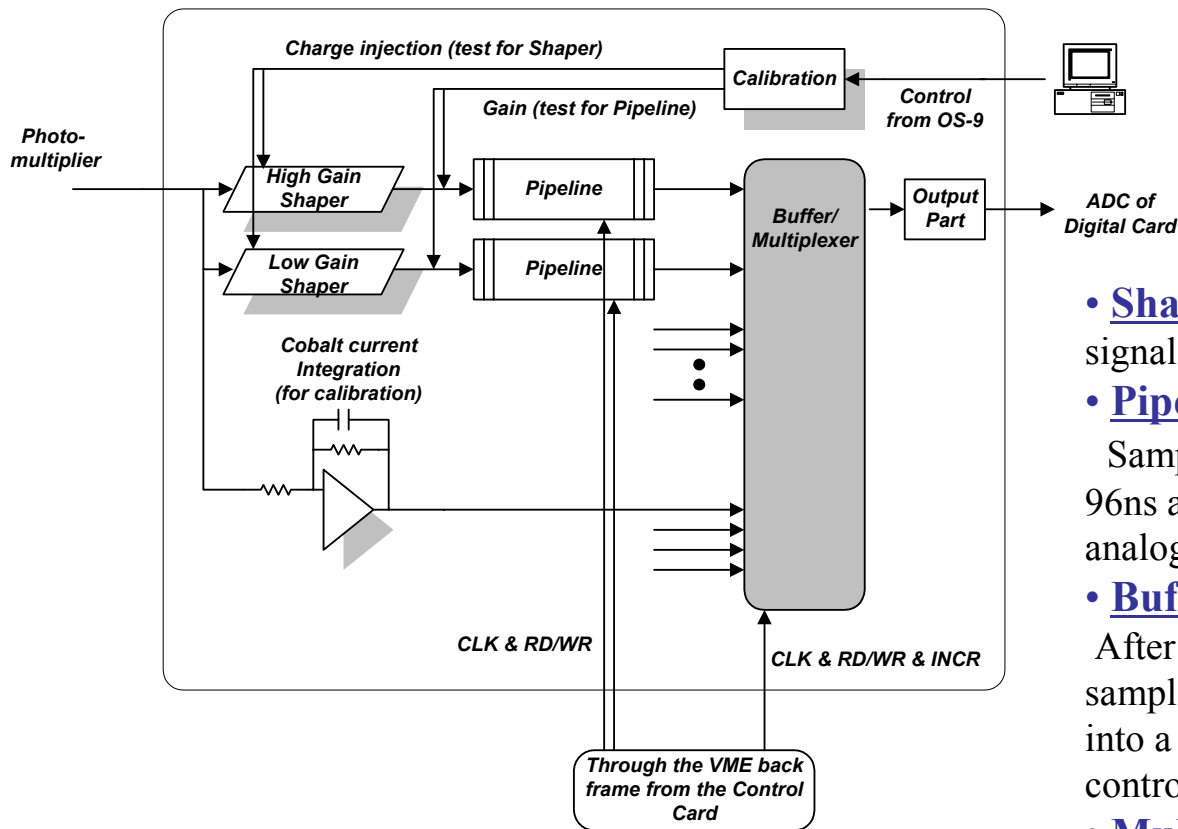
$$\text{with small mass } (E \simeq |p|)$$

- Lead(1.5 cm)-scintillator(0.26 cm) sandwich calorimeter
- For electrons
 $\sigma(E)/E = (0.41 \pm 0.02)/\sqrt{E} \oplus (0.062 \pm 0.002)$
- For pions (FPC+FCAL)
 $\sigma(E)/E = (0.65 \pm 0.02)/\sqrt{E} \oplus (0.06 \pm 0.01)$
- Installation in 20x20cm² beam hole of FCAL.
 - ✓ Extend calorimetric acceptance by 1 unit in pseudorapidity from $\eta_{\max}=4$ to $\eta_{\max}=5$.

Forward Plug Calorimeter Readout Scheme



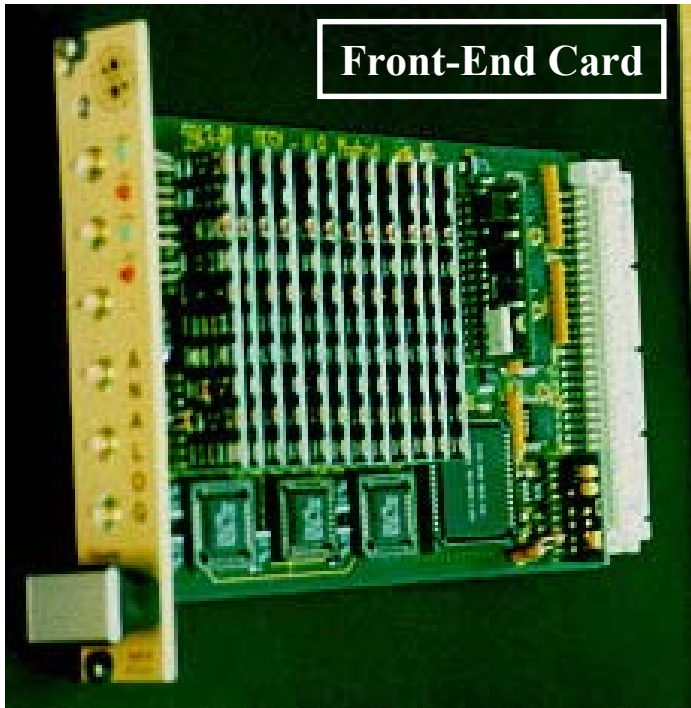
Front-End Electronics : Analog card



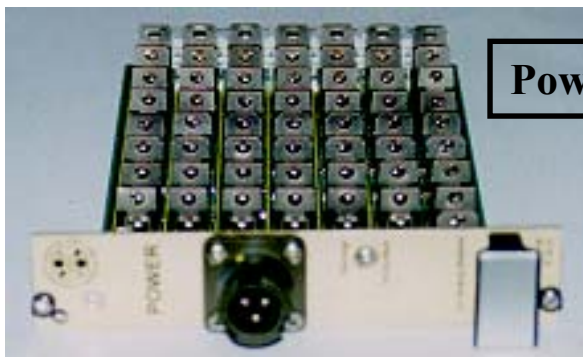
- **Shaper** : Amplify and shape the signals from PMTs.
- **Pipeline** : (1 signal = 8 samples)
Sample the shaped signal per 96ns and store them in a 5 μ s deep analog pipeline.
- **Buffer** :
After GFLT's decision, the 8 samples per channel are carried into a buffer and wait for the control signal from a Multiplexer.
- **Multiplexer** : Convert the parallel-input into serial-output.
- **Output Driver** : Transfer the signals to ADC over the 60 m cable.

- Follow the readout scheme of ZEUS calorimeter.
- Energy range \rightarrow 1:7000 (from 0.03 GeV to 200 GeV for EMC)
 - ✓ Difficult for 12 bit ADC to digitize the signal.
 - \rightarrow Process the signals with low and high gain.

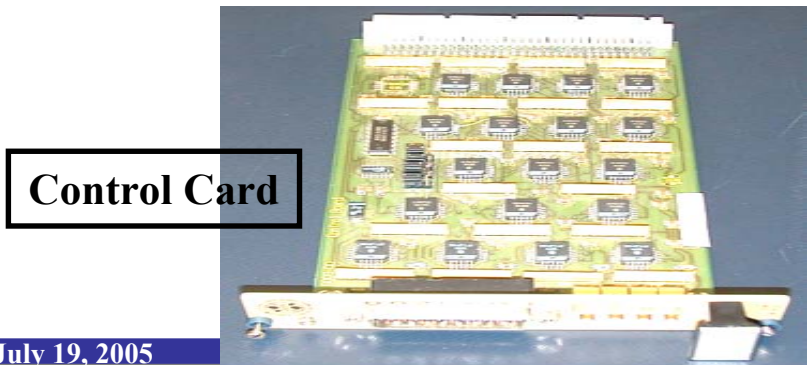
Front-End Electronics



Front-End Card

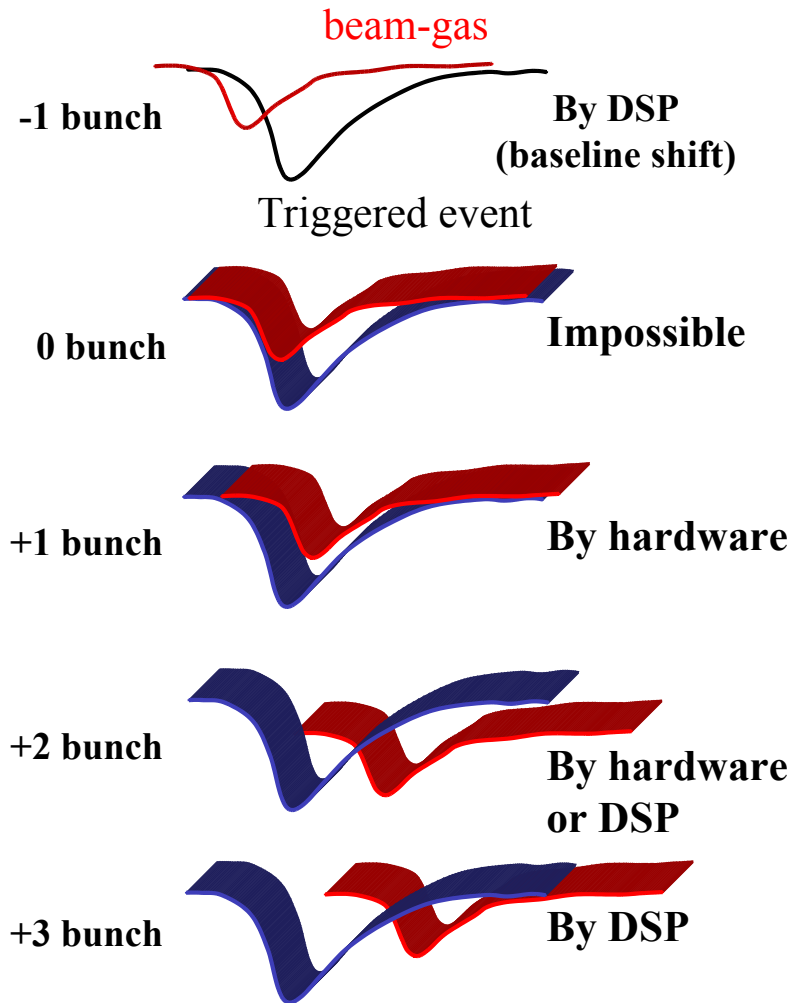


Power Card



Control Card

Pile-up Rejection Card



- In order to measure the charge and time of a signal from a PMT accurately,
→ Signal is amplified and shaped.

- If a signal has the time width longer than the beam crossing interval of 96 ns, it may be distorted by an event produced at an earlier (later) bunch leading to pile-up.

- Need to check this effect for the FPC located near to the beam-hole.

- Pile-up Rejection Card (PRC)
→ Identify the pile-up due to beams of -1, +1 or +2 bunch by checking the timing of input signal

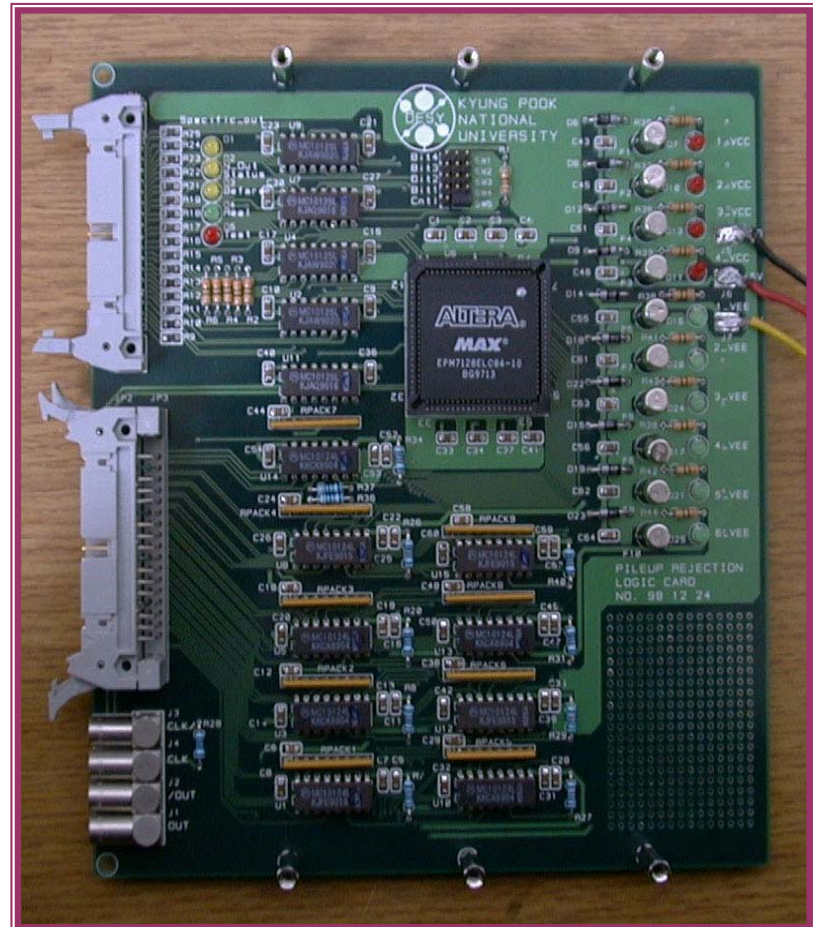
- PRC shows that **events below 0.2 %** of the triggered physics events are affected by pile-up effect.

Pile-up Rejection Card

PRC Analog Card
installed on Detector

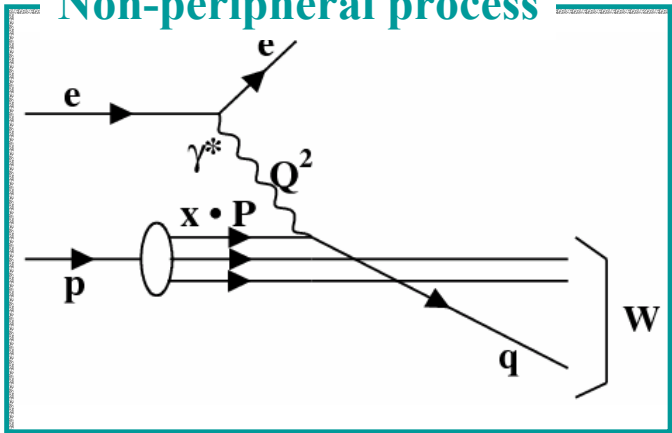


PRC Logic Card installed in Rucksack



Inclusive Diffraction in Deep Inelastic Scattering

Non-peripheral process



Kinematics of $ep \rightarrow eXp$

$$Q^2 = -(k - k')^2$$

$$x = Q^2 / (2q \cdot p)$$

$$W = \sqrt{(p + q)^2} = \sqrt{y \cdot s}$$

$$M_X^2 = (k - k' + p - p')^2$$

$$x_{IP} \approx \frac{Q^2 + M_X^2}{Q^2 + W^2}$$

$$\beta \approx \frac{Q^2}{M_X^2 + Q^2} = \frac{x}{x_{IP}}$$

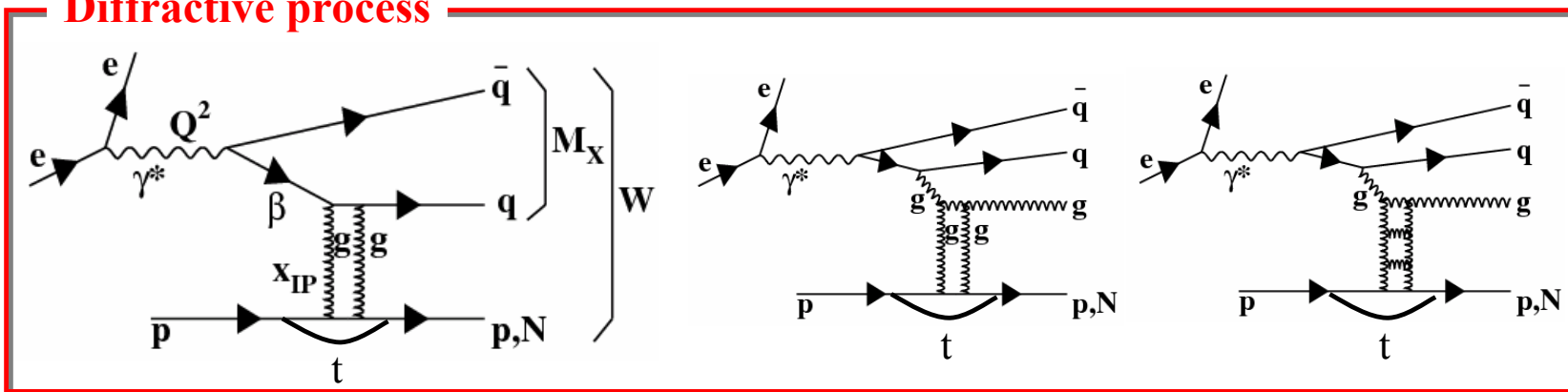
$$t = (p - p')^2$$

$$x_L = p'_Z / E_p = 1 - x_{IP}$$

Present diffractive measurement in terms of

$$\rightarrow d\sigma(M_X, W, Q^2) / dM_X \text{ and } x_{IP} F_2^{D(3)}(\beta, x_{IP}, Q^2)$$

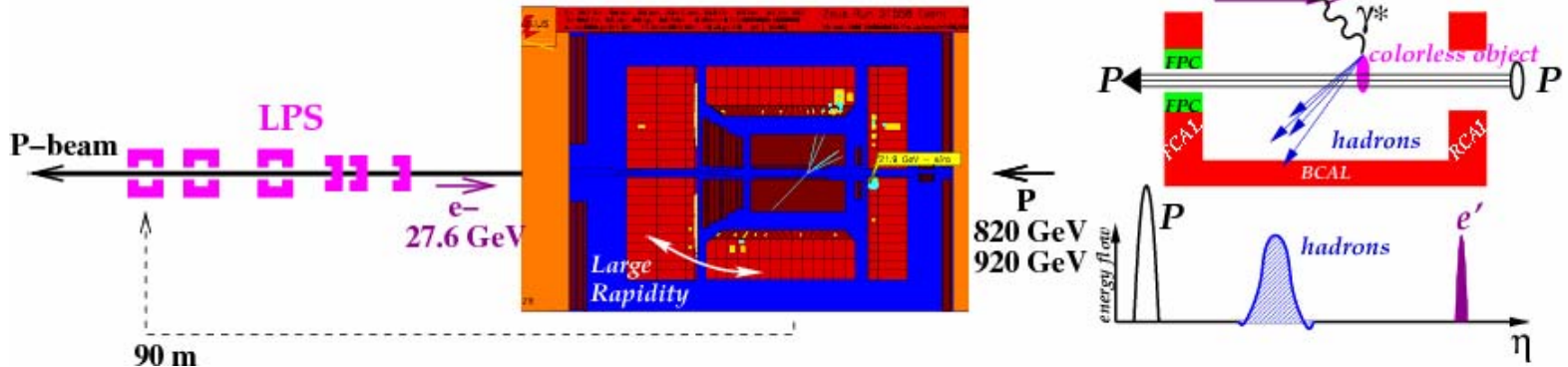
Diffractive process



Event Topologies ($ep \rightarrow eXp$)

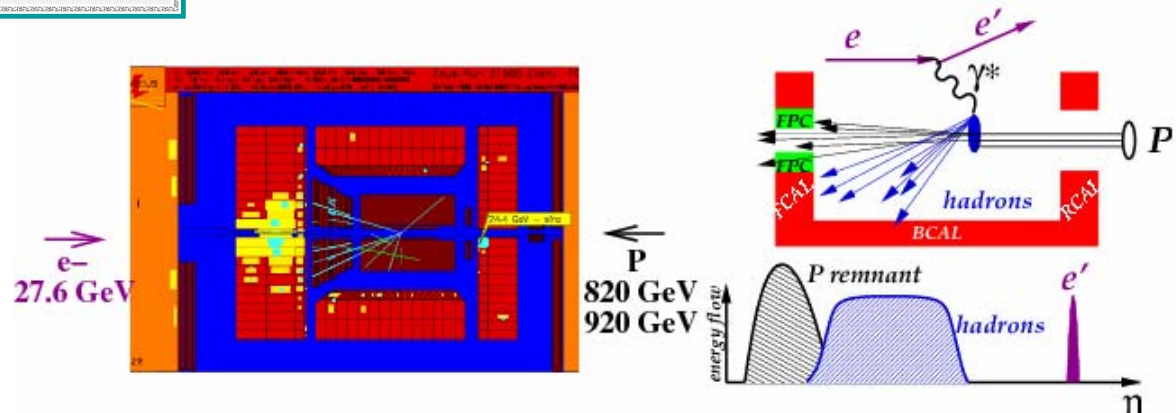
Diffractive scattering

($M_X = 5 \text{ GeV}$, $Q^2 = 19 \text{ GeV}^2$, $W = 123 \text{ GeV}$)



Non-peripheral scattering

($M_X = 45 \text{ GeV}$, $Q^2 = 13 \text{ GeV}^2$, $W = 93 \text{ GeV}$)

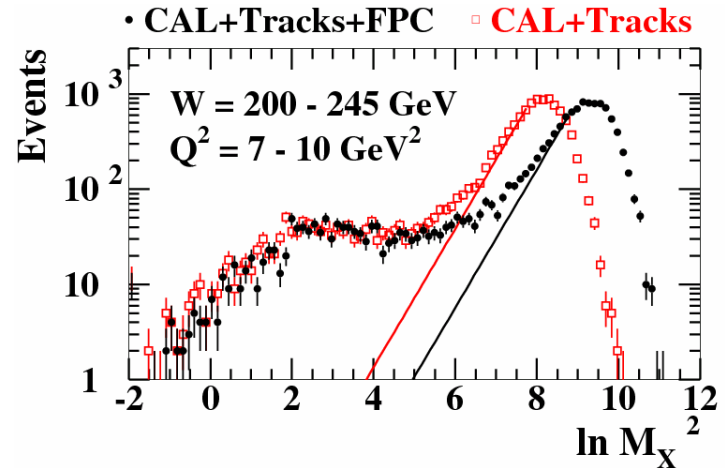
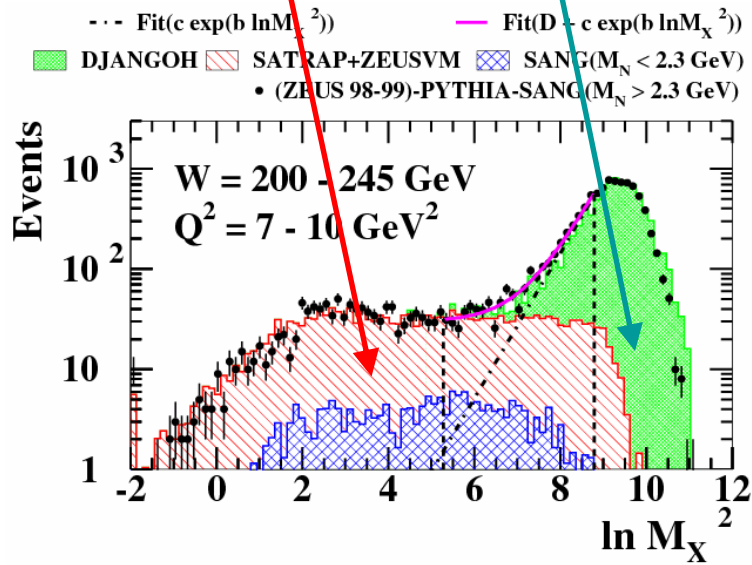


M_X method using Forward Plug Calorimeter

$$\frac{dN}{d \ln M_X^2} = \underbrace{D}_{\text{Diffraction}} + \underbrace{c \cdot \exp(b \cdot \ln M_X^2)}_{\text{Non-diffraction}}$$

Diffraction **Non-diffraction**

with free parameters, D , b and c from fit.



- ✓ The FPC increases the accessible M_X range by a factor of 1.7.
- ✓ If $M_N > 2.3 \text{ GeV}$ deposits $E_{\text{FPC}} > 1 \text{ GeV}$,
 → recognized and rejected

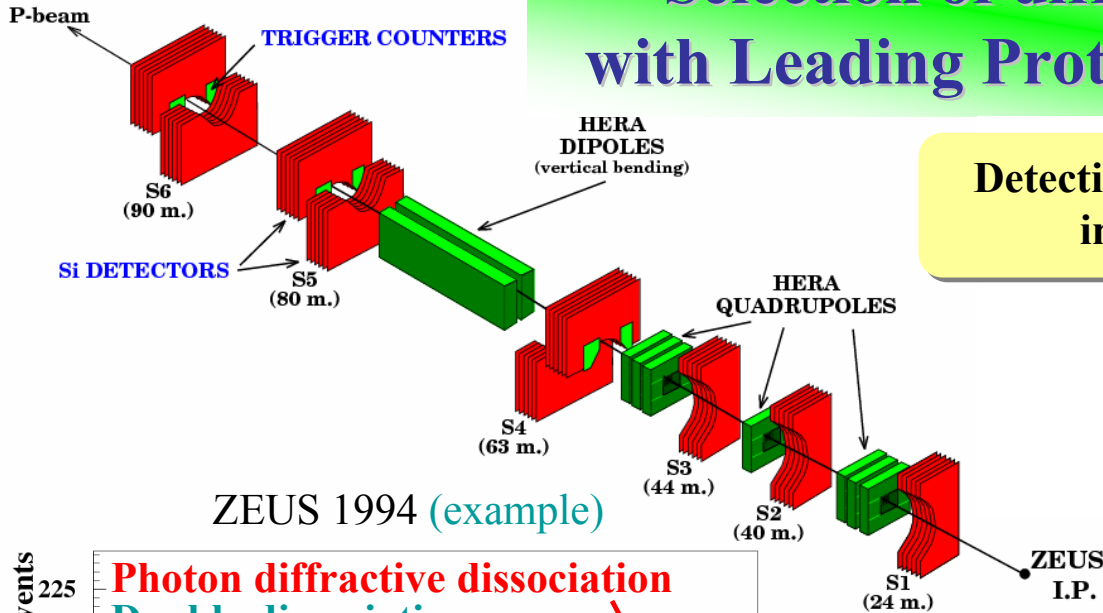
$$d\sigma_{\gamma^* p \rightarrow XN}^{\text{diff}} / dM_X, M_N < 2.3 \text{ GeV}$$

- $2.2 < Q^2 < 80 \text{ GeV}^2$
- $37 < W < 245 \text{ GeV}$
- $0.28 < M_X < 35 \text{ GeV}$

Using 98-99 data
with 4.2 pb^{-1}

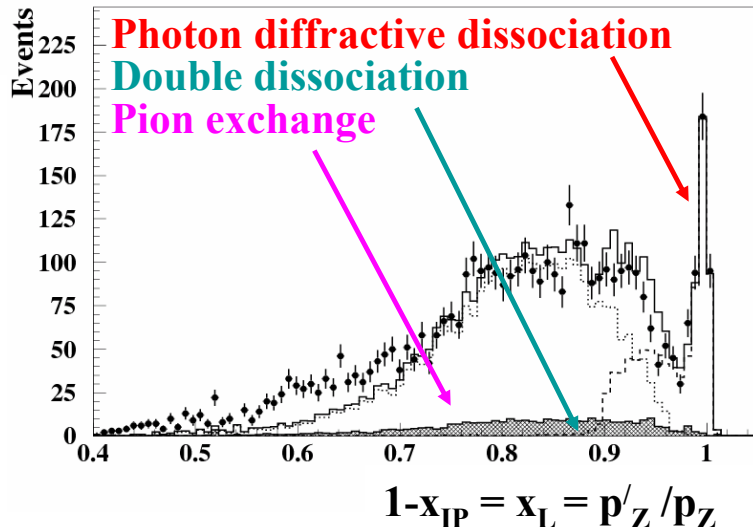
Nucl. Phys. **B713**, 3 (2005)

Selection of diffractive events with Leading Proton Spectrometer



Detection of the scattered proton in LPS with $x_L > 0.9$.

ZEUS 1994 (example)



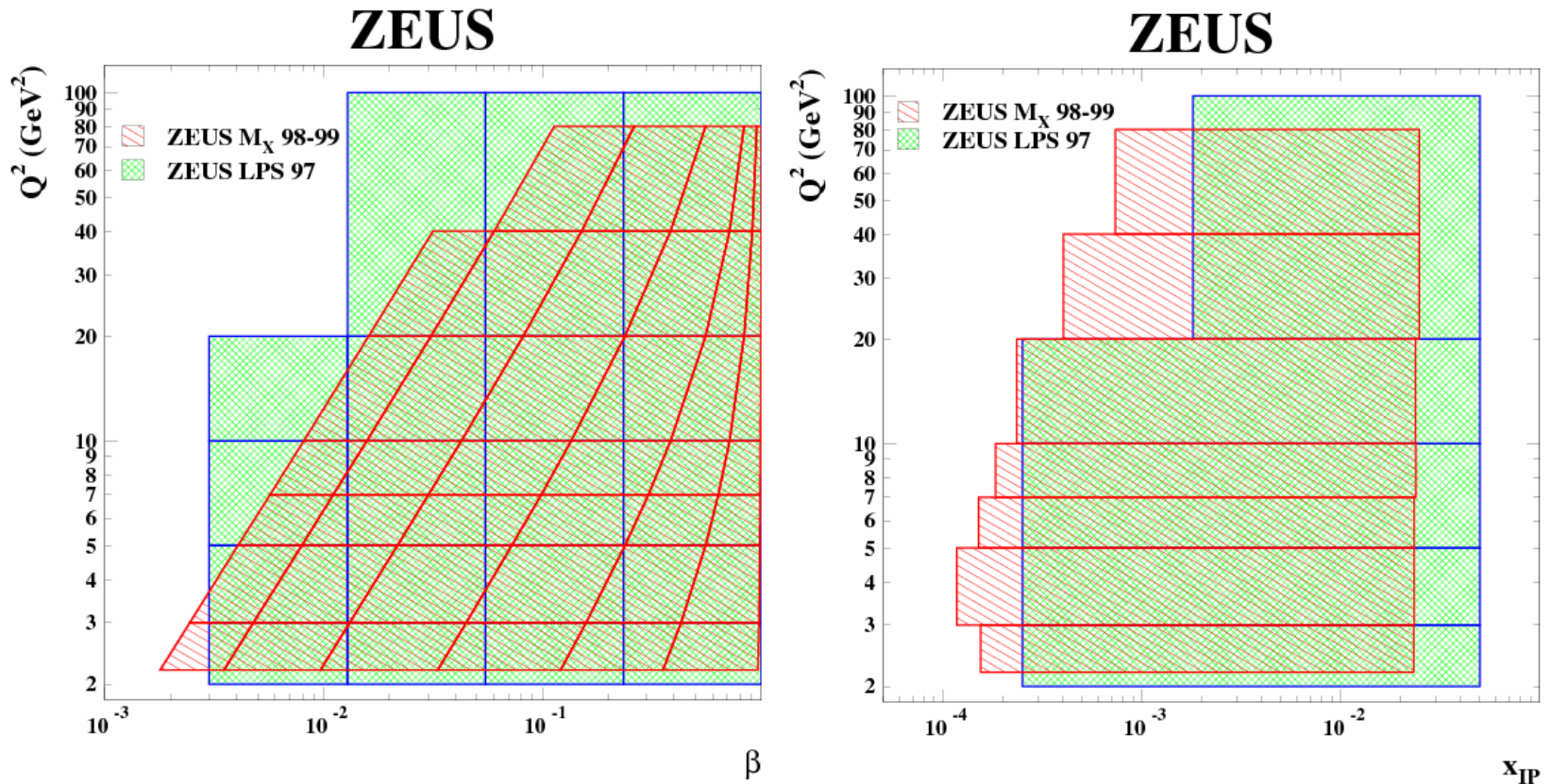
- ✓ No background from proton dissociation.
- ✓ Limited statistics due to geometrical acceptance $\sim 2\%$ in the diffractive peak region.

$$d\sigma_{\gamma^* p \rightarrow XN}^{\text{diff}} / dM_X dt \quad \text{Using 97 data}$$

- $0.03 < Q^2 < 0.60 \text{ GeV}^2 \rightarrow 3.6 \text{ pb}^{-1}$
- $2 < Q^2 < 100 \text{ GeV}^2 \rightarrow 12.8 \text{ pb}^{-1}$
- $25 < W < 280 \text{ GeV}$
- $1.5 < M_X < 70 \text{ GeV}$
- $0 < |t| < 1 \text{ GeV}^2$

Eur. Phys. J. C38, 43 (2004)

Kinematical ranges



- **M_X method** : Lower M_X region (~ higher β region) and lower x_{IP} region.
- **LPS method** : Higher x_{IP} region

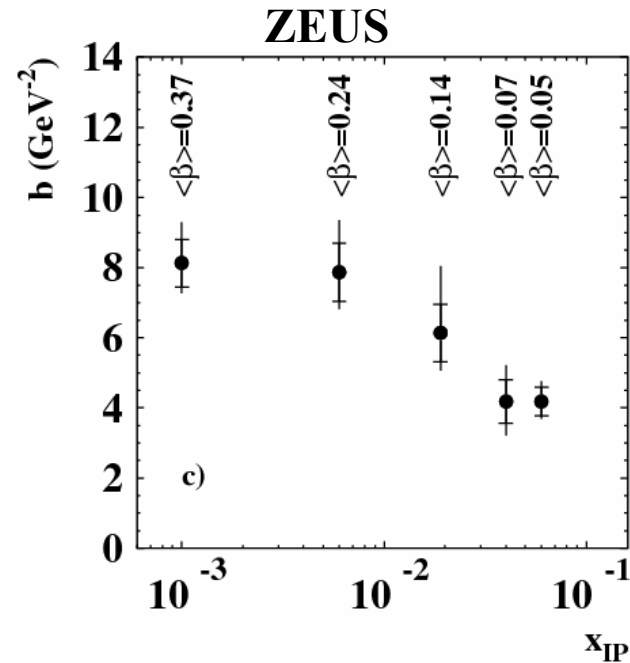
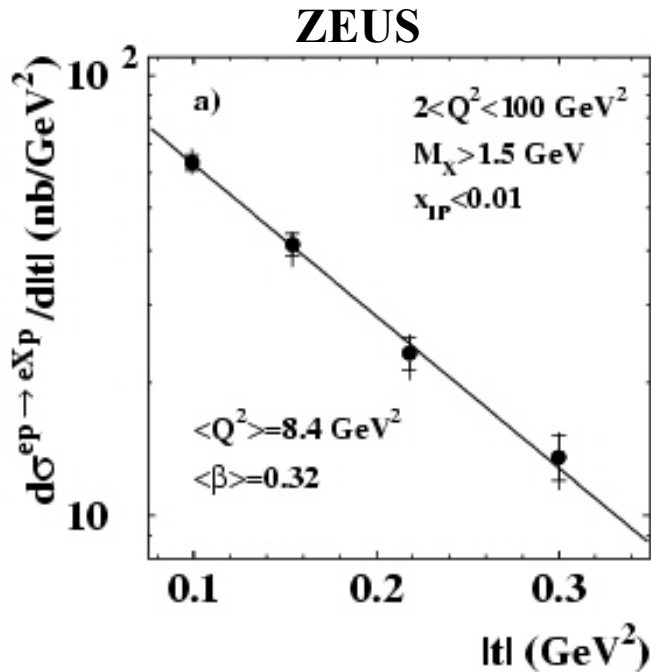
Diffractive Cross Section

- **t dependence**
- **W dependence**
→ $\alpha_{\text{IP}}^{\text{diff}}(0)$
- **M_X dependence**
- $\sigma^{\text{diff}}/\sigma^{\text{tot}}$

Diffractive Structure Function

- **x_{IP} dependence**
→ Q^2 dependence
- **Comparison with theory**
- **β dependence**

t dependence of Diffractive Cross Section (LPS)



- Fit t distribution to $d\sigma/d|t| \propto \exp(-b|t|)$

$$b = 7.9 \pm 0.5(\text{stat.})_{-0.5}^{+0.9}(\text{syst.})\text{GeV}^{-2}$$

→ $d\sigma/d|t|$ shows steep fall-off with t as in elastic hadron-hadron scattering.

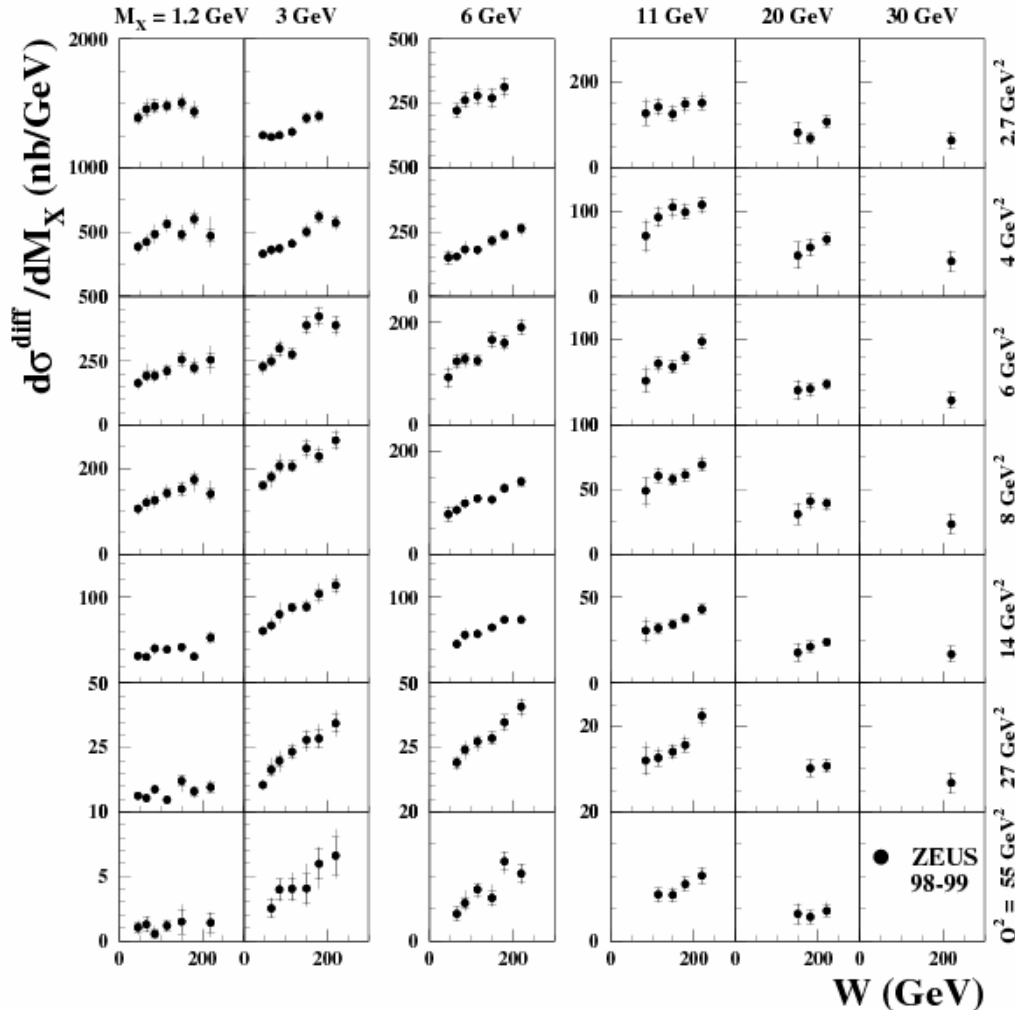
- **Regge phenomenology predicts “shrinkage” of the diffractive peak:**

$$b = b_0 + 2\alpha' \ln \frac{W^2}{M_X^2} \approx b_0 + 2\alpha'_{IP} \ln \frac{1}{x_{IP}}$$

- Additional β dependence expected in models.

Diffractive Cross Section (M_X)

ZEUS

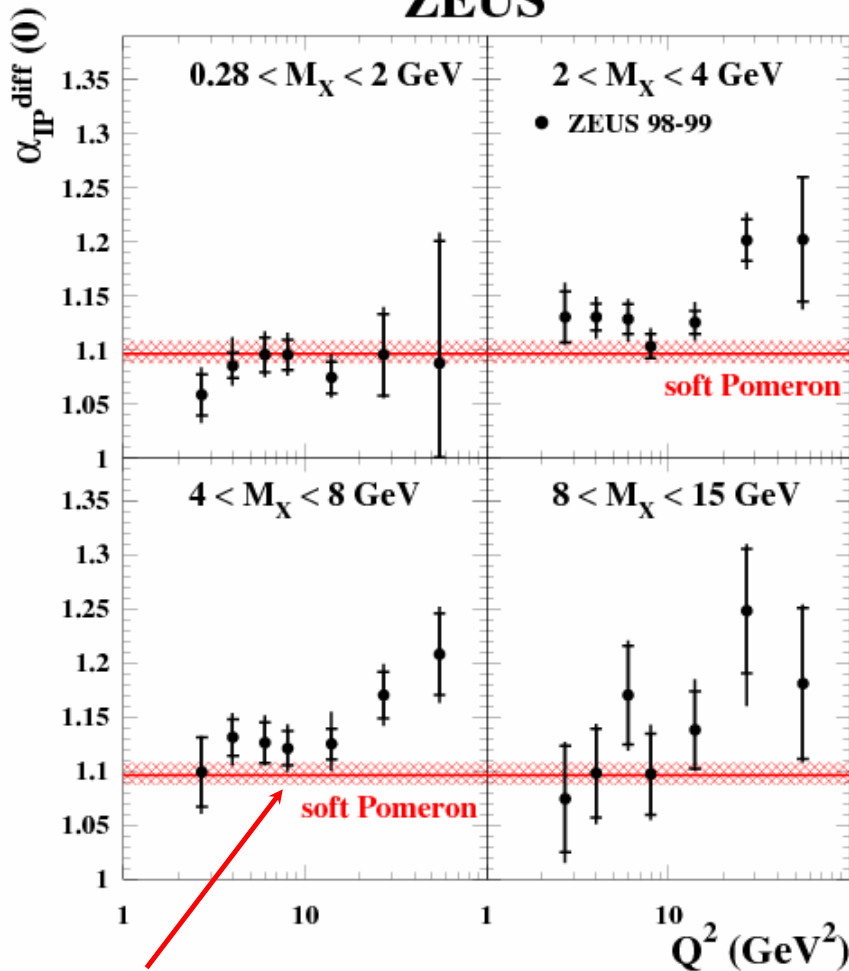


$$d\sigma^{\text{diff}}_{\gamma^* p \rightarrow XN} / dM_X, M_N < 2.3 \text{ GeV}$$

- For $M_X < 2 \text{ GeV}$, $d\sigma/dM_X$ depends weakly on W .
- For $M_X > 2 \text{ GeV}$, $d\sigma/dM_X$ rises rapidly with W .

W dependence of Diffractive Cross Section

ZEUS



$$\alpha_{\text{IP}}^{\text{soft}}(0) = 1.096^{+0.012}_{-0.009} \text{ from had-had scattering}$$

- Fit to the diffractive cross section :

$$\frac{d\sigma^{\text{diff}}}{dM_X} = h \cdot W^{a^{\text{diff}}} \sim (W^2)^{(2\bar{\alpha}_{\text{IP}}-2)}$$

(h, a^{diff} free parameters)

Assuming $d\sigma/dt \propto e^{b \cdot t}$ and

$$\alpha_{\text{IP}}(t) = \alpha_{\text{IP}}(0) + \alpha'_{\text{IP}} \cdot t$$

$$\therefore \alpha_{\text{IP}}(0) = \bar{\alpha}_{\text{IP}} + \underbrace{\alpha'_{\text{IP}}/b}_{\text{from LPS}} \approx (a^{\text{diff}}/4 + 1) + \underbrace{0.03}$$

- For M_X < 2 GeV

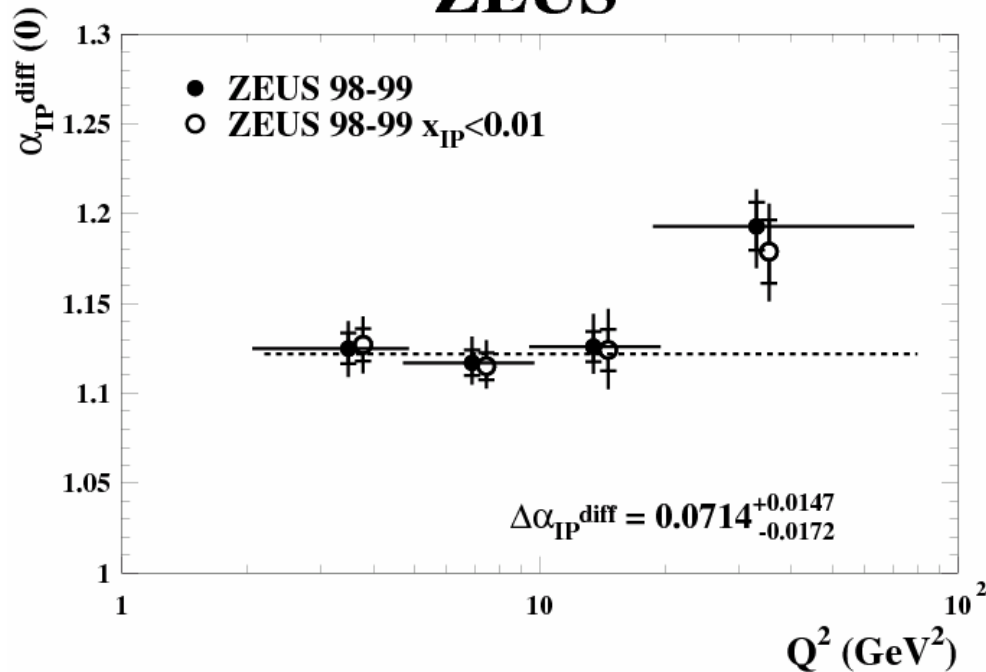
→ $\alpha_{\text{IP}}^{\text{diff}}(0)$ compatible with the soft Pomeron.

- For larger M_X and Q² > 20 GeV²

→ $\alpha_{\text{IP}}^{\text{diff}}(0)$ lies above the results expected from soft Pomeron and increases with Q².

Q² dependence of $\alpha_{\text{IP}}^{\text{diff}}(0)$

ZEUS



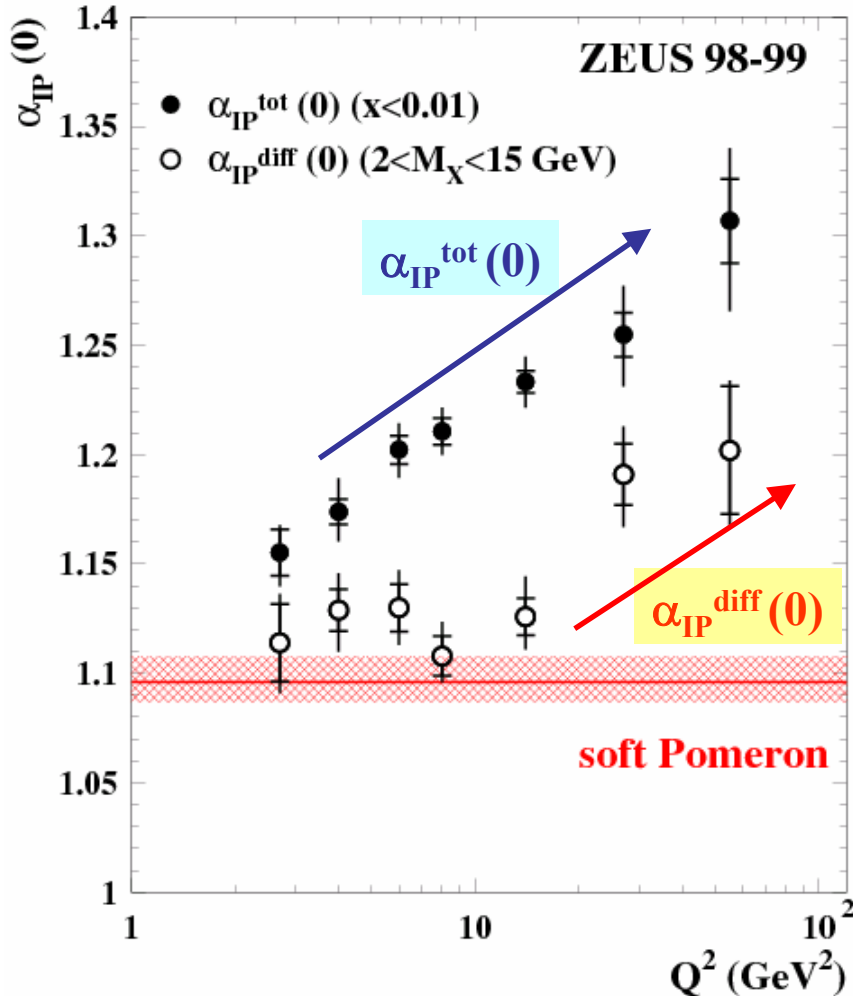
- Fit to data with $2 < M_X < 15 \text{ GeV}$

$$\begin{aligned} \Delta\alpha_{\text{IP}}^{\text{diff}} &\equiv \alpha_{\text{IP}}^{\text{diff}}(0; 2.7 < Q^2 < 20 \text{ GeV}^2) \\ &\quad - \alpha_{\text{IP}}^{\text{diff}}(0; 20 < Q^2 < 80 \text{ GeV}^2) \\ &= \underline{0.0714 \pm 0.0140(\text{stat.})^{+0.0047}_{-0.0100}(\text{syst.})} \end{aligned}$$

- ✓ $\alpha_{\text{IP}}^{\text{diff}}(0)$ is rising with Q^2 , with a significance of 4.2 s.d.
- ✓ Assuming single Pomeron exchange, this observation contradicts Regge factorisation.

Compare α_{IP} for diffractive and total γ^*p scattering

ZEUS



$$\sigma_{\gamma^*p}^{tot} = \frac{4\pi^2\alpha}{Q^2(1-x)} F_2(x, Q^2)$$

$$\sim \frac{1}{W^2} \text{Im} T_{\gamma^*p \rightarrow \gamma^*p}(W^2, t=0)$$

$$\sim (W^2)^{\alpha_{IP}^{tot}(0)-1}$$

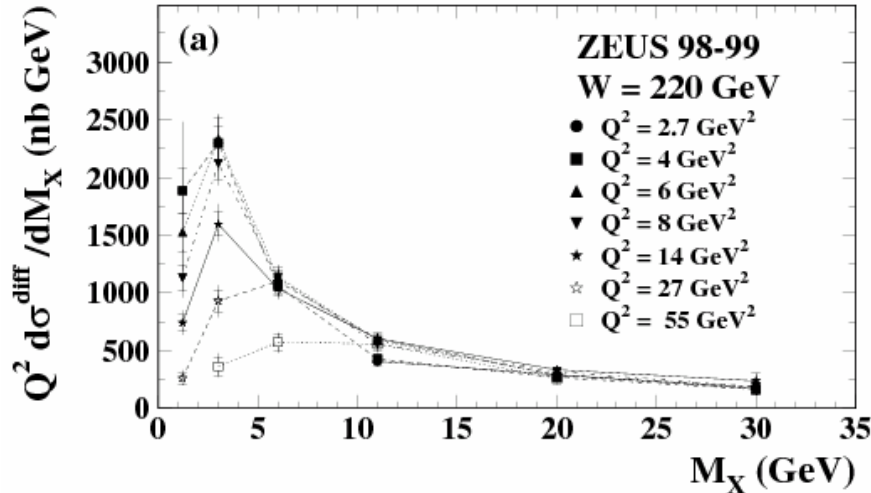
$$\frac{d^2\sigma_{\gamma^*p}^{diff}}{dM_X dt} = |T_{\gamma^*p \rightarrow \gamma^*p}|^2 \sim (W^2)^{2(\alpha_{IP}^{diff}(0)-1)}$$

- $\alpha_{IP}^{diff}(0)$ is lower than for $\alpha_{IP}^{tot}(0)$.
- For low Q^2 , $\alpha_{IP}^{diff}(0)$ is consistent with soft Pomeron.
- Data suggest increase with Q^2 .
 - Regge factorisation breaking.
 - Similar W dependence of diffractive and inclusive measurement,

$$2(\alpha_{IP}^{diff}(0)-1) \approx \alpha_{IP}^{tot}(0) - 1$$

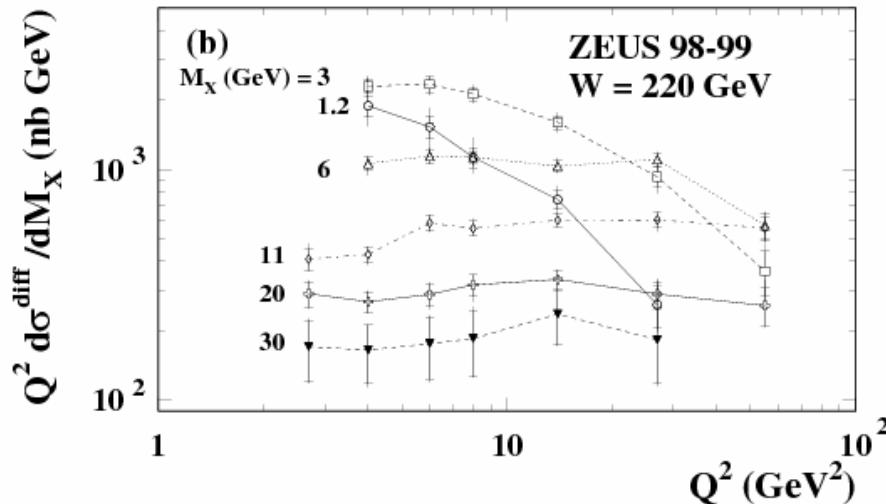
M_X dependence of diffractive cross section

ZEUS

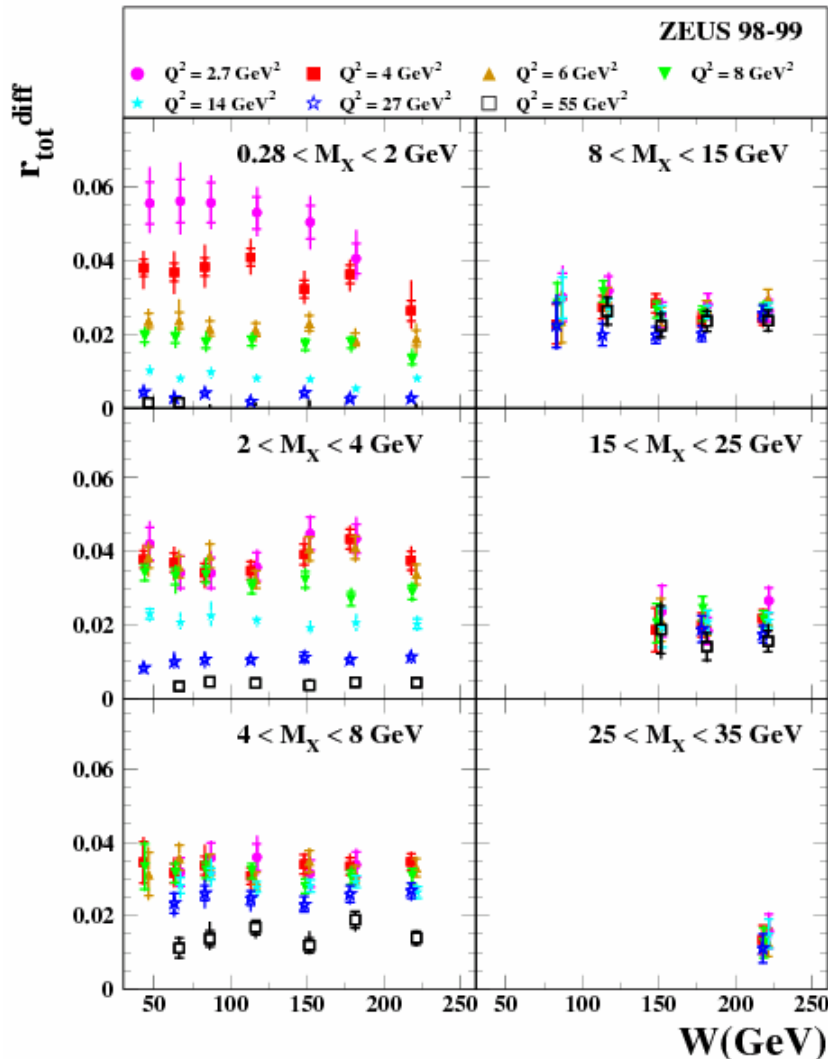


$$Q^2 \cdot \frac{d\sigma^{\text{diff}}}{\gamma^* p \rightarrow XN} \text{ vs. } M_X \text{ at } W = 220 \text{ GeV}$$

- For $M_X < 4 \text{ GeV}$,
rapid decrease with Q^2 .
→ predominantly higher twist.
- For $M_X > 10 \text{ GeV}$,
constant or slow rise with Q^2 .
→ leading twist.



Diffraction contribution of the total cross section



$$R_{\text{tot}}^{\text{diff}} = \frac{\int_{M_a}^{M_b} dM_X d\sigma_{\gamma^* p \rightarrow XN, M_N < 2.3 \text{ GeV}}^{\text{diff}} / dM_X}{\sigma_{\gamma^* p}^{\text{tot}}} \propto \frac{(W^2)^{2\alpha_{\text{IP}} - 2}}{(W^2)^{\alpha_{\text{IP}}(0) - 1}}$$

- For $M_X < 2 \text{ GeV}$, falling with W .
- For $M_X > 2 \text{ GeV}$, constant with W .
- For $M_X < 4 \text{ GeV}$, decreasing with rising Q^2 .
- For $M_X > 8 \text{ GeV}$, no Q^2 dependence.

- For the highest W bin ($200 < W < 245 \text{ GeV}$), $\sigma^{\text{diff}}(0.28 < M_X < 35 \text{ GeV}, M_N < 2.3 \text{ GeV}) / \sigma^{\text{tot}}$

$$15.8_{-1.0}^{+1.2} \% \quad \text{at } Q^2 = 4 \text{ GeV}^2$$

$$9.6_{-0.7}^{+0.7} \% \quad \text{at } Q^2 = 27 \text{ GeV}^2$$

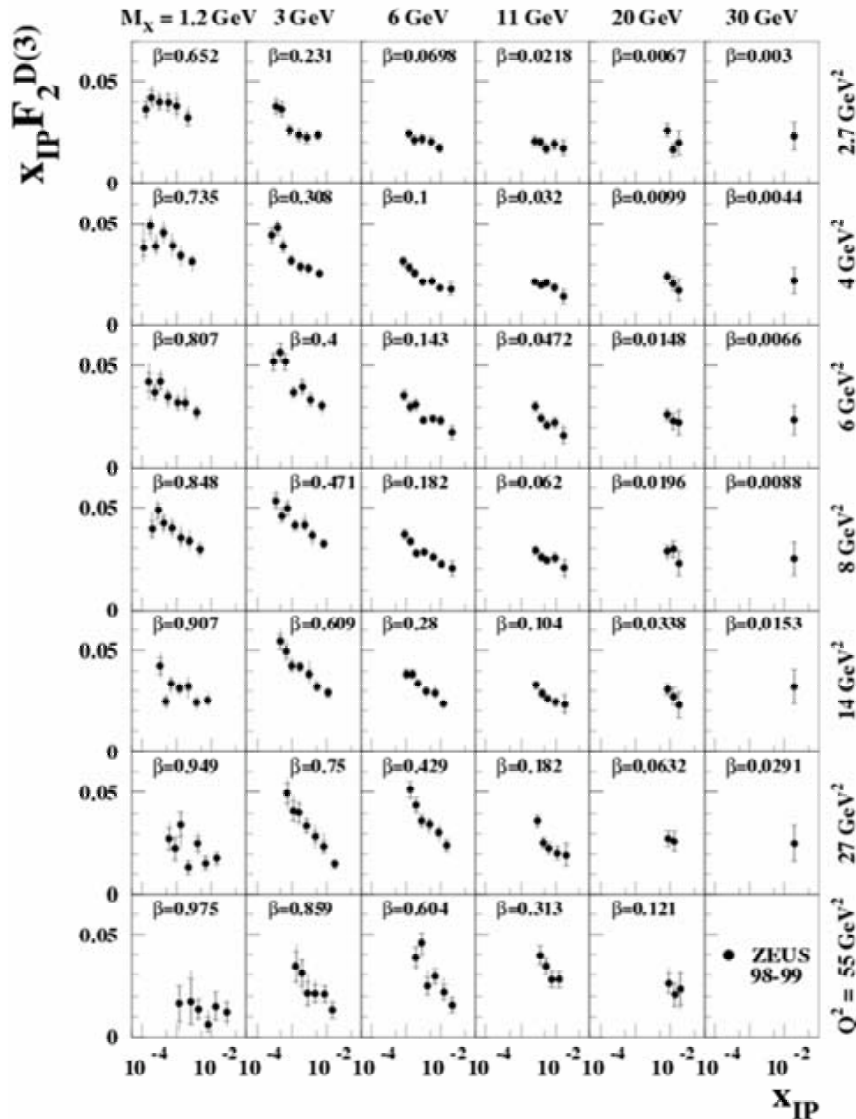
Diffractive Cross Section

- **t dependence**
- **W dependence**
→ $\alpha_{\text{IP}}^{\text{diff}}(0)$
- **M_X dependence**
- $\sigma^{\text{diff}}/\sigma^{\text{tot}}$

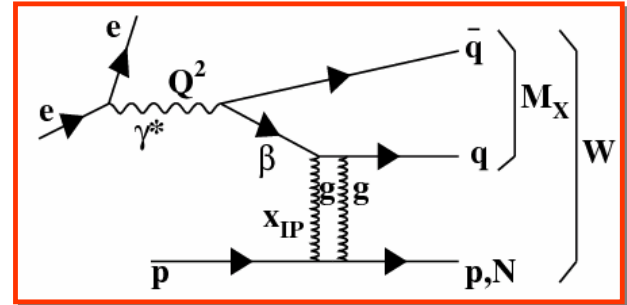
Diffractive Structure Function

- **x_{IP} dependence**
→ Q^2 dependence
- **Comparison with theory**
- **β dependence**

ZEUS



Diffractive structure function of proton



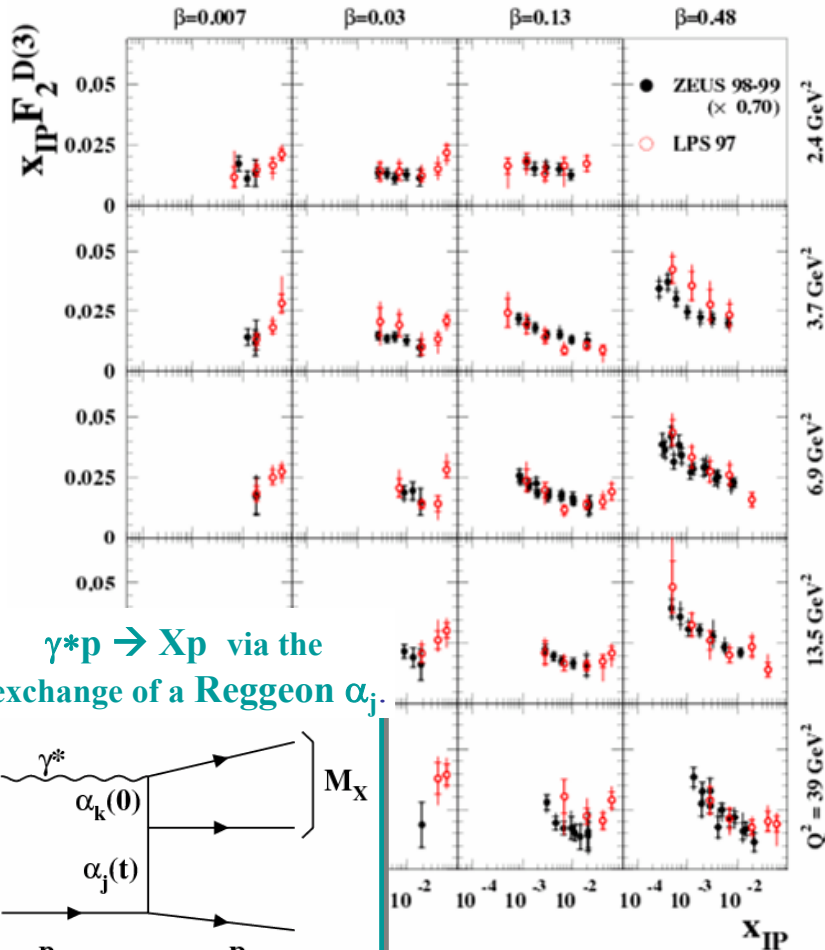
$$X_{IP} F_2^{D(3)}(\beta, x_{IP}, Q^2) =$$

$$\frac{1}{4\pi^2 \alpha} \cdot \frac{Q^2 (Q^2 + M_X^2)}{2M_X} \cdot \frac{d\sigma_{\gamma^* p \rightarrow XN}^{diff}}{dM_X}$$

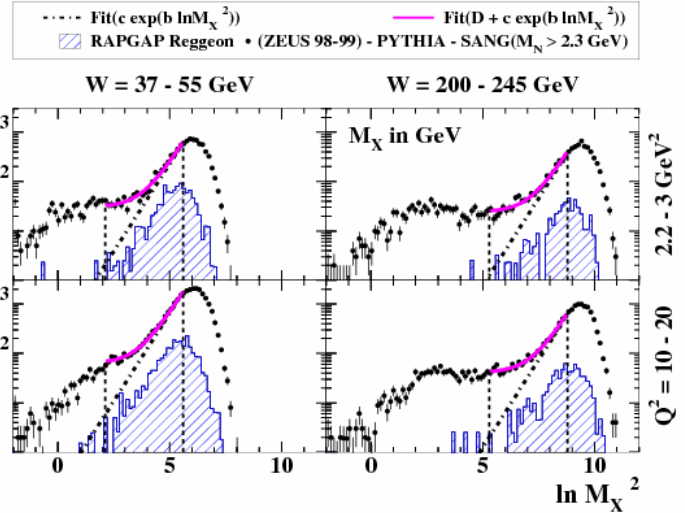
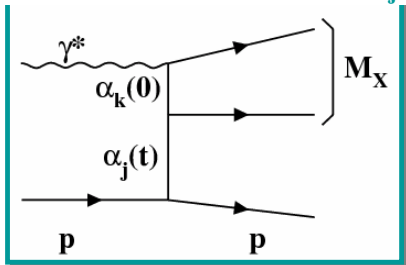
- **For $M_X < 2 \text{ GeV}$,**
 $x_{IP} F_2^{D(3)}$ is constant with x_{IP} .
- **For $M_X > 2 \text{ GeV}$,**
 rapid increase as $x_{IP} \rightarrow 0$.
 i.e. parton evolution as $x_{IP} \rightarrow 0$.

Comparison of LPS and M_X method

ZEUS



$\gamma^* p \rightarrow Xp$ via the exchange of a Reggeon α_j .



$$\frac{d\sigma_{\text{Reggeon}}^{\gamma^* p \rightarrow XN}}{d \ln M_X^2} \propto \exp\left[(1 + \alpha_k(0) - 2\bar{\alpha}_j) \cdot \ln M_X^2\right]$$

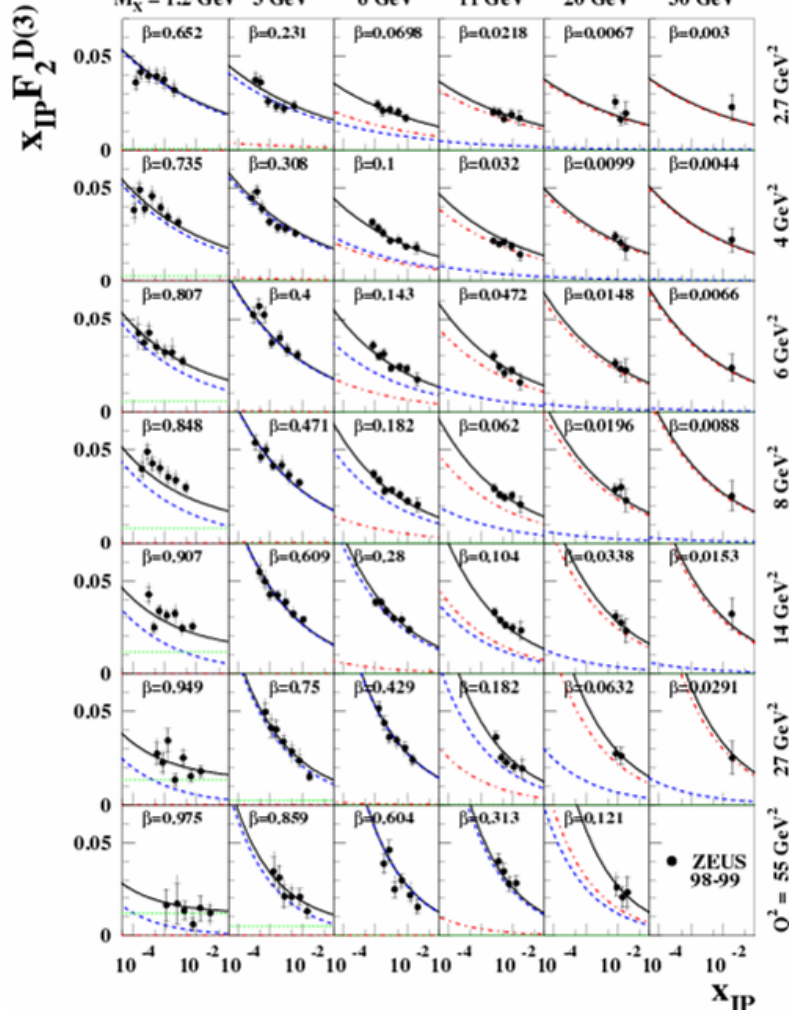
$$\propto \exp(b_{\text{IR}} \cdot \ln M_X^2) \text{ with } b_{\text{IR}} = 1$$

- M_X method suppresses the Reggeon contributions.
- Good agreement between LPS and M_X method ($\times 0.7$ for $M_N < 2.3$ GeV) except for the region of $x_{\text{IP}} > 0.01$ where Reggeon contributions may dominate LPS.

Comparison with colour dipole model, BEKW

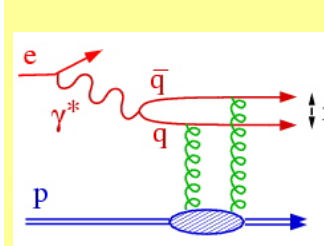
BEKW(mod) : — Total ···· $(q\bar{q})_T$ ····· $(q\bar{q})_L$ ····· $(q\bar{q}g)_T$
 $M_X = 1.2 \text{ GeV}$ 3 GeV 6 GeV 11 GeV 20 GeV 30 GeV

(Bartels, Ellis, Kowalski and Wüsthoff)



- The BEKW parametrisation describes the data, well.

$$x_{IP} F_2^{D(3)} = c_T \cdot F_{q\bar{q}}^T + c_L \cdot F_{q\bar{q}}^L + c_g \cdot F_{q\bar{q}g}^T$$

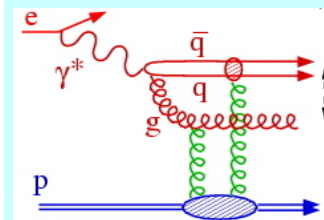


$$F_{q\bar{q}}^T \propto \beta(1 - \beta)$$

dominates at $\beta > 0.15$

$$F_{q\bar{q}}^L \propto \beta^3(1 - 2\beta)^2$$

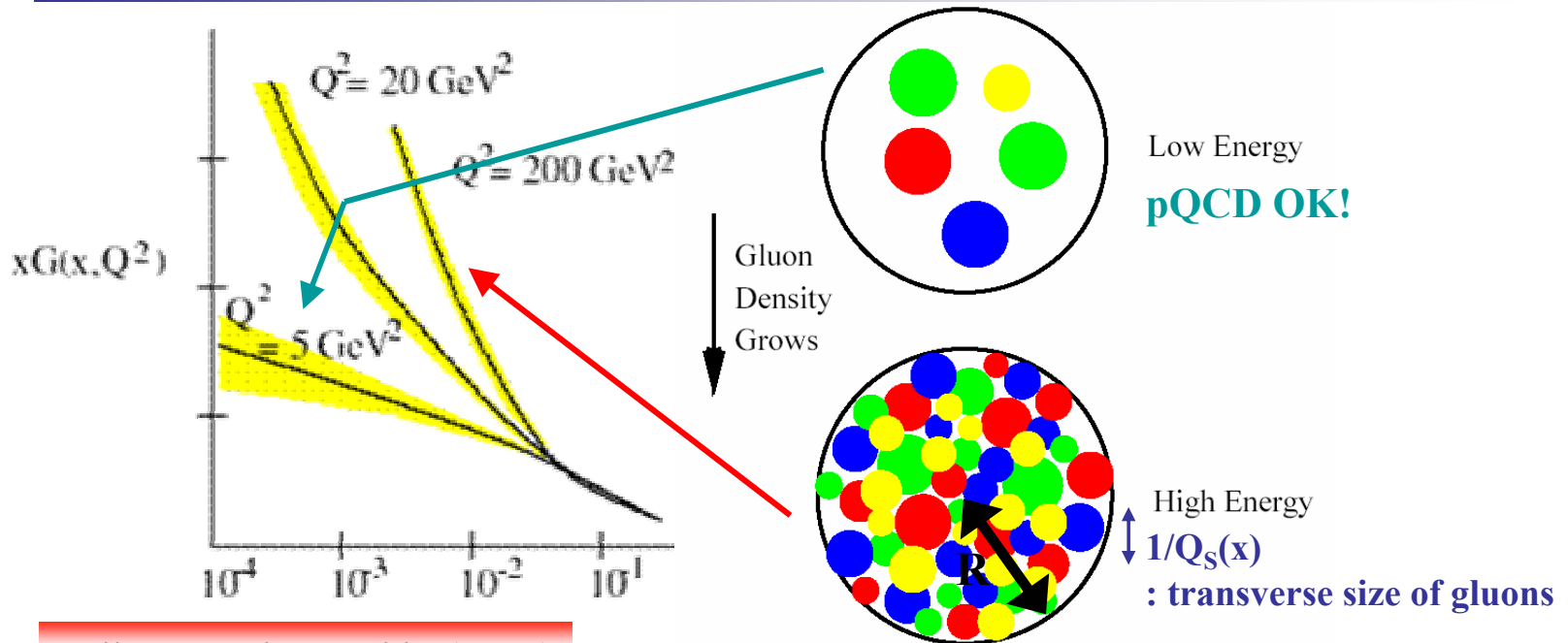
substantial at large β



$$F_{q\bar{q}g}^T \propto (1 - \beta)^\gamma$$

dominates at small β

High gluon density and saturation



Gribov, Levin, Ryskin (1984)

At small x , QCD evolution

- predicts a fast increase of the parton densities which violate unitarity constraints.
- neglect interactions between partons.

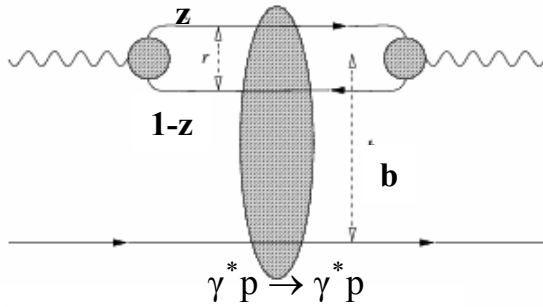
But, not be valid for the high parton density.

When **high gluon density**, gluons start to overlap (the proton “saturates”.)

- ✓ They are not “free” anymore and interact each other.
- ✓ F_2 stops growing.

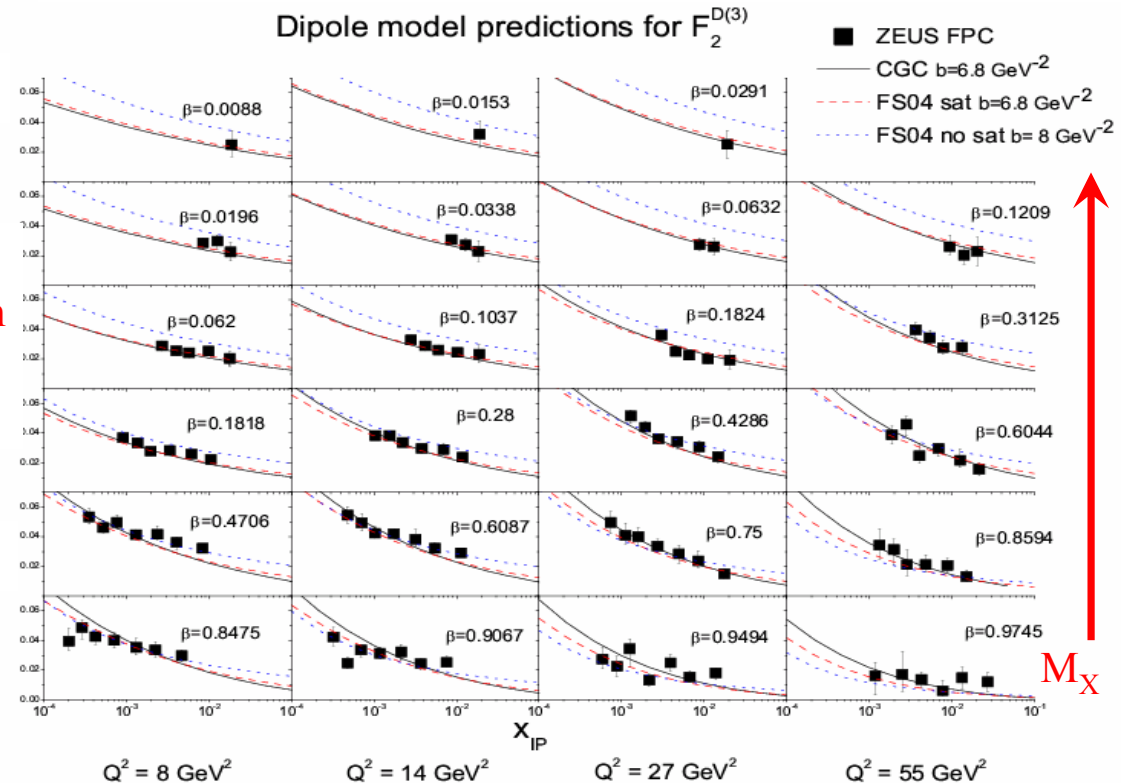
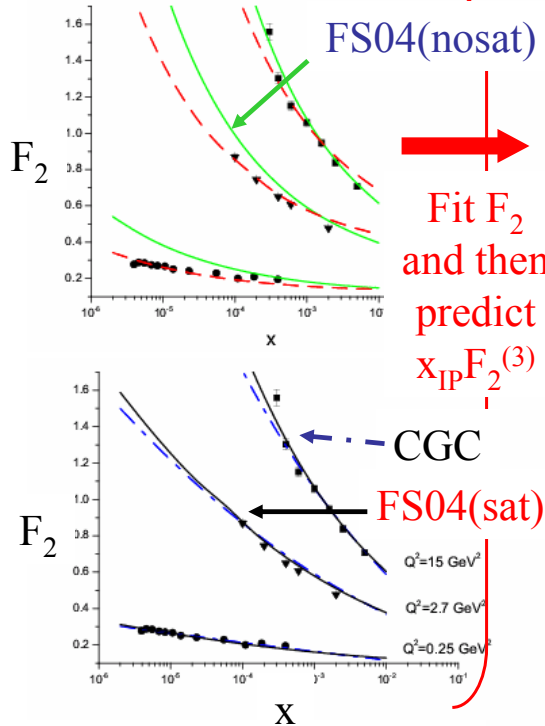
→ **non-linear equation is required.**

Comparison with colour dipole model, saturation

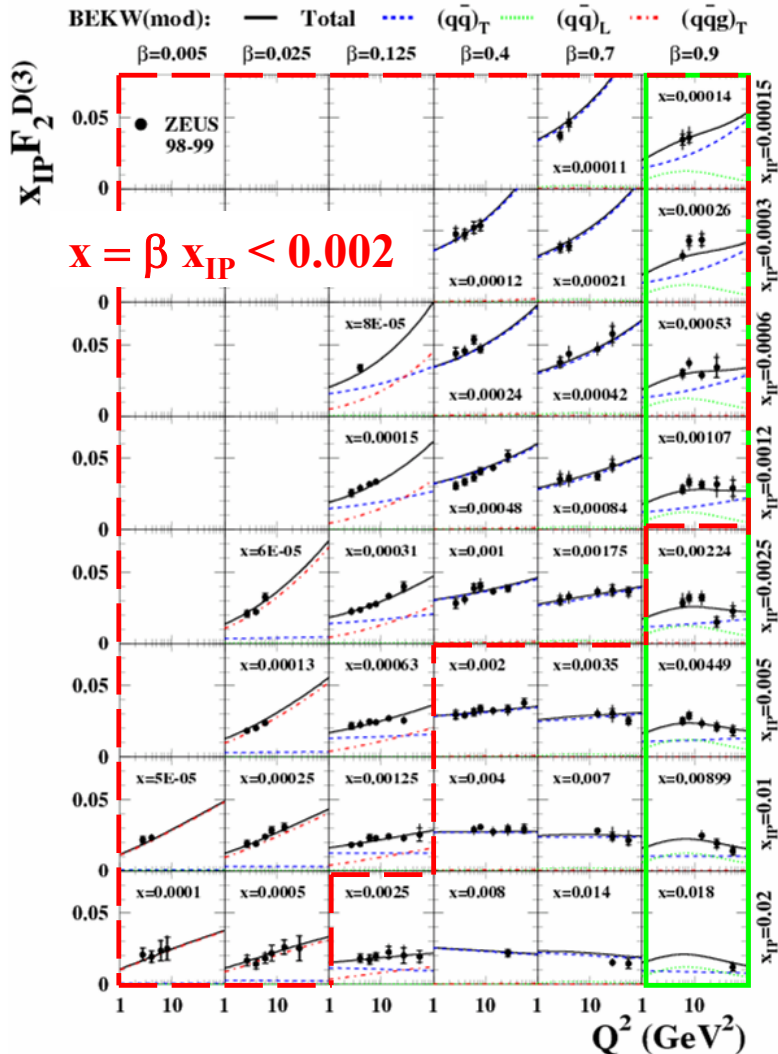


Comparison with Forshaw and Shaw (FS04) model with/without saturation (hep-ph/0411337) and Colour Glass Condensate (CGC) model from Iancu, Itakura, Munier (hep-ph/0310338).

→ CGC and FS04(sat) are able simultaneously to describe F_2 and $x_{IP}F_2D^{(3)}$.



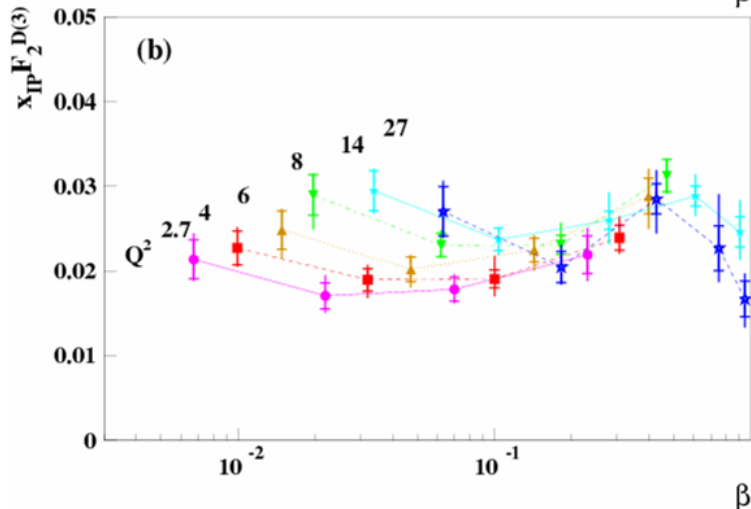
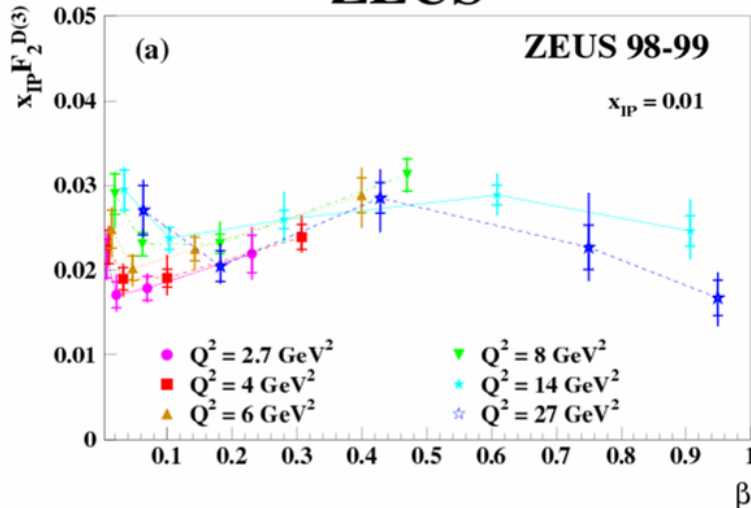
Q^2 dependence of $x_{IP}F_2^{D(3)}$



- For $\beta=0.9$
 - (dominated by events with $M_X < 2$ GeV),
 - Constant or slowly decreasing with Q^2 .
 - Expect higher twist effect from $(q\bar{q})_L$.
- For $\beta \leq 0.7$ and $x = \beta x_{IP} < 0.002$,
 - $x_{IP}F_2^{D(3)}$ increases with increasing Q^2 .
 - **Positive scaling violations.**
 - Suggest perturbative effects such as gluon emission
- For fixed β ,
 - Q^2 dependence of $x_{IP}F_2^{D(3)}$ changes with x_{IP} .
 - **Inconsistent with the Regge factorisation hypothesis**

β dependence of $x_{IP}F_2^{D(3)}$ at $x_{IP}=0.01$

ZEUS



- $x_{IP}F_2^{D(3)}$ for $x_{IP}=x_0=0.01$
 → expect this to represent **the structure function of Pomeron**, up to a normalisation constant.

- **For $\beta > 0.1$**

$x_{IP}F_2^{D(3)}$ has a maximum around $\beta=0.5$.

→ The **$\beta(1-\beta)$ dependence observed is expected in dipole models** of diffraction by $\gamma^* \rightarrow q\bar{q}$ splitting and two gluon exchange.

- **For $\beta < 0.1$**

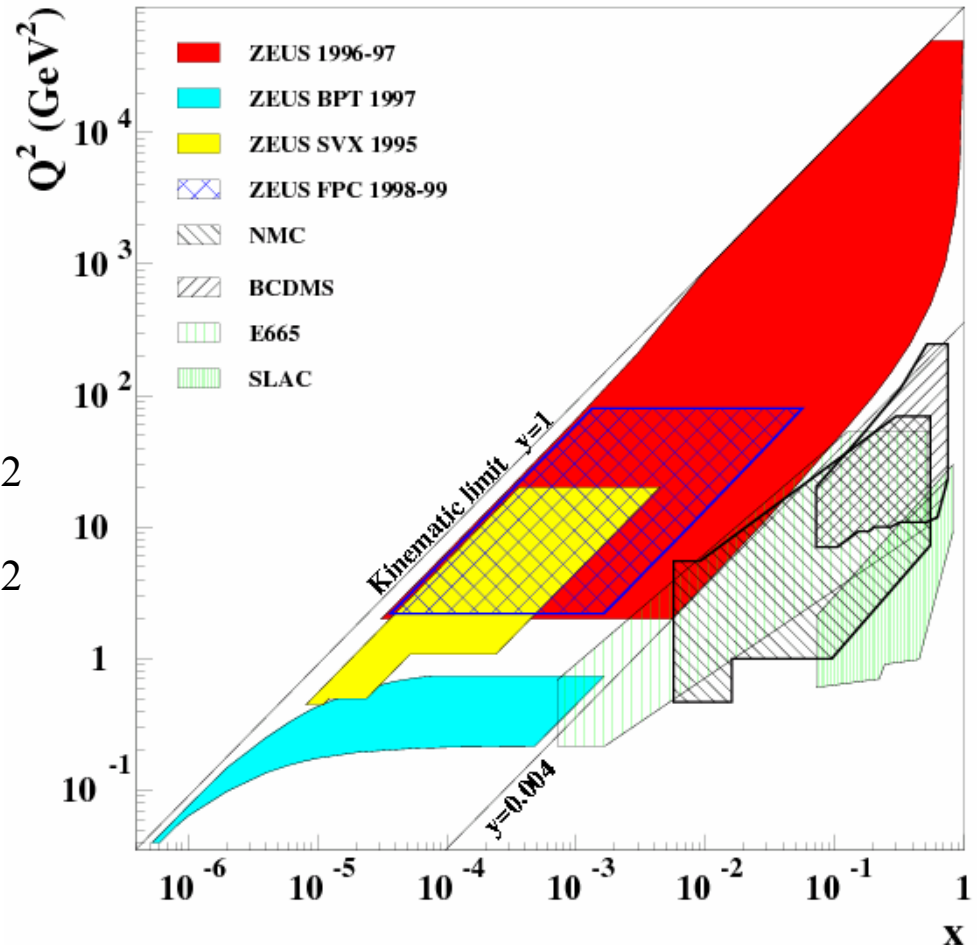
$x_{IP}F_2^{D(3)}$ rises as $\beta \rightarrow 0$ and the rise accelerates with growing Q^2 .

→ Similar to **the logarithmic scaling violation of F_2 at low x** due to QCD evolution.

Phenomenology of F_2

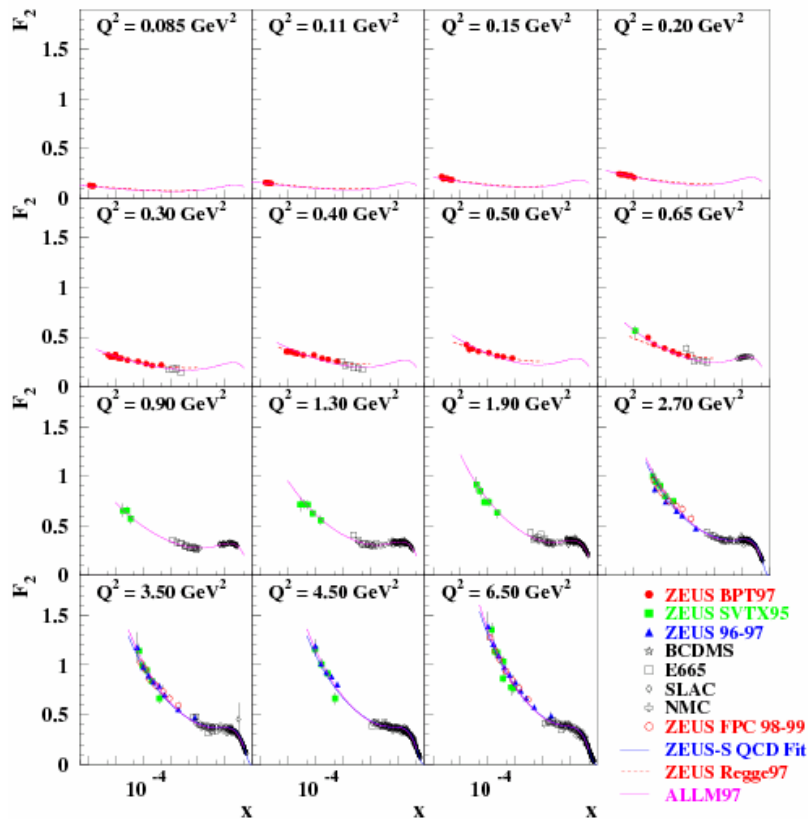
Phenomenological studies of F_2 measured in a large kinematic range

- Logarithmic derivative of F_2 with respect to x
- Logarithmic derivative of F_2 with respect to Q^2

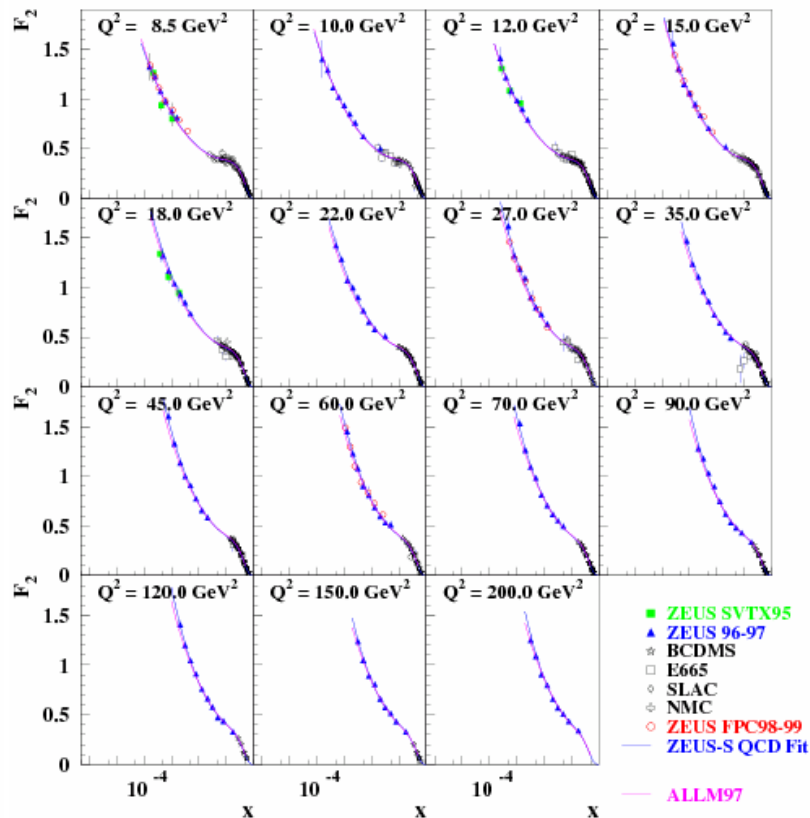


F₂ measurement

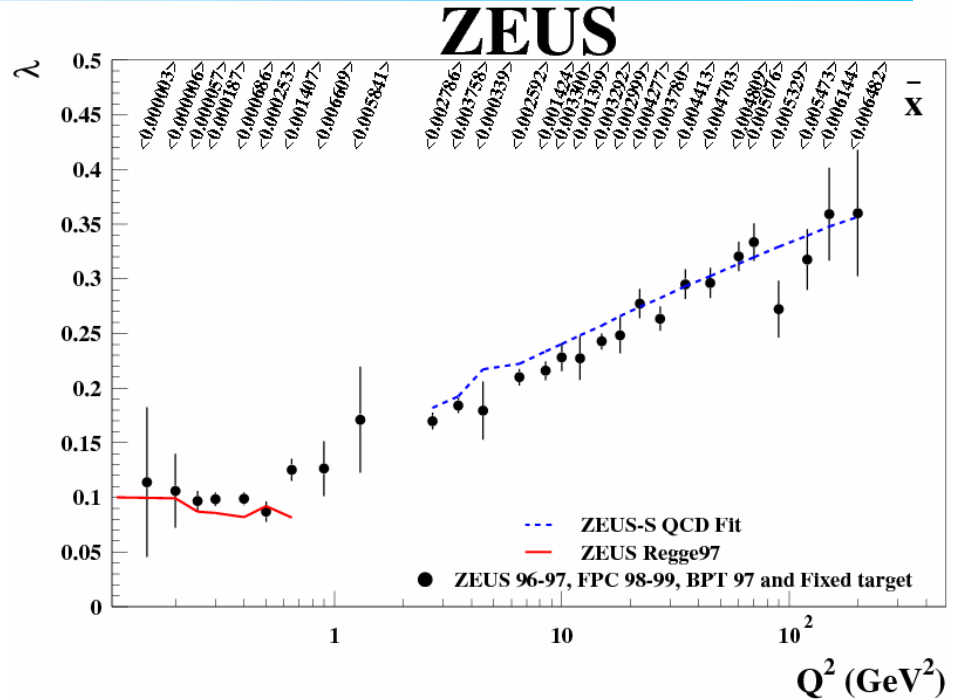
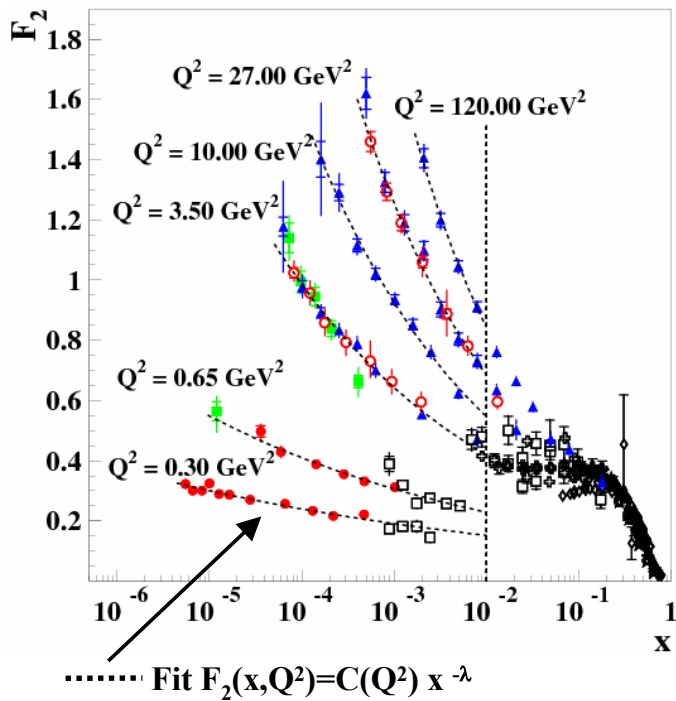
ZEUS



ZEUS



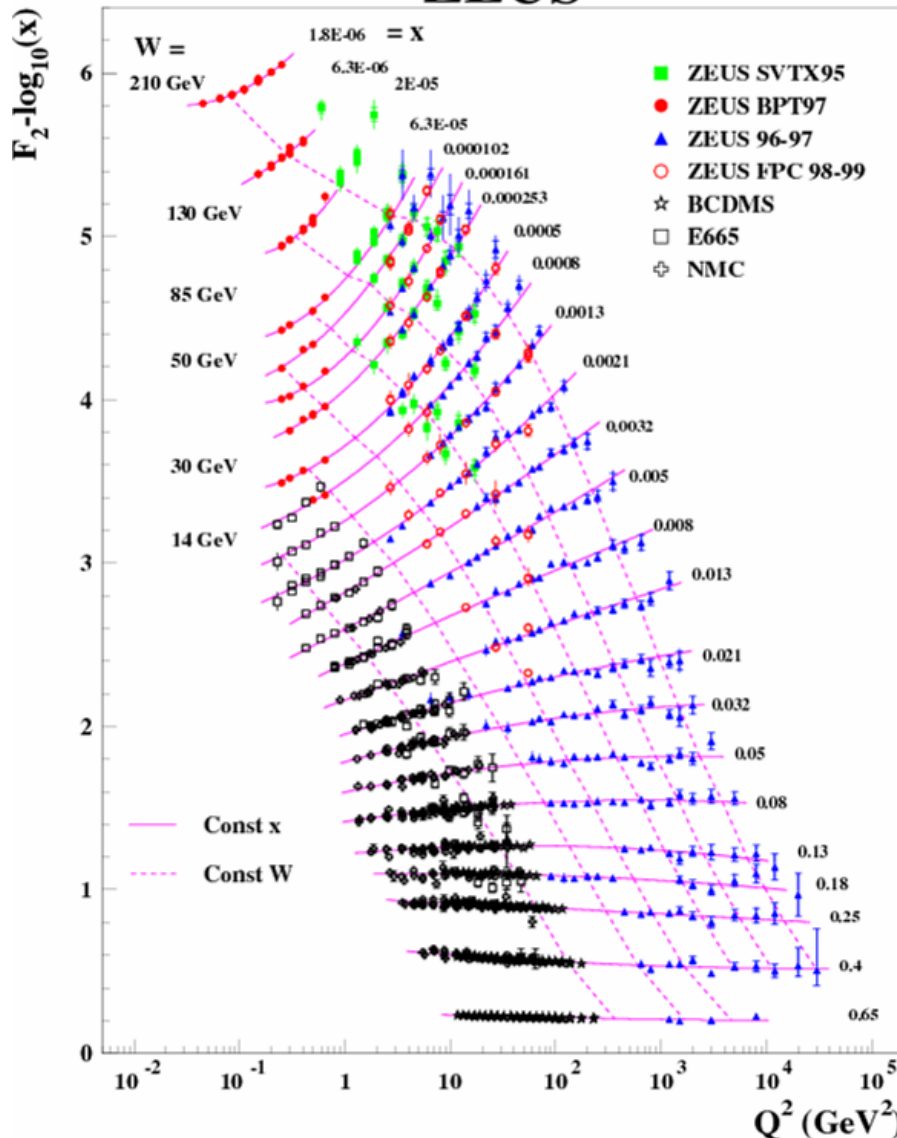
F₂ slopes : dF₂/dln(1/x) at fixed Q²



- Rise of F₂ with x increases with Q².
 - ➔ Quantify this behaviour from the slope $dF_2/d\ln(1/x) = \lambda$
 - ➔ Fit $F_2(x, Q^2) = C(Q^2) x^{-\lambda}$ to the data with $x < 0.01$ in bins of Q².

- For Q² > 2.7 GeV², λ increases ~ lnQ² .
- For Q² < 0.6 GeV², λ ~ 0.1 is consistent with the prediction of soft Pomeron.

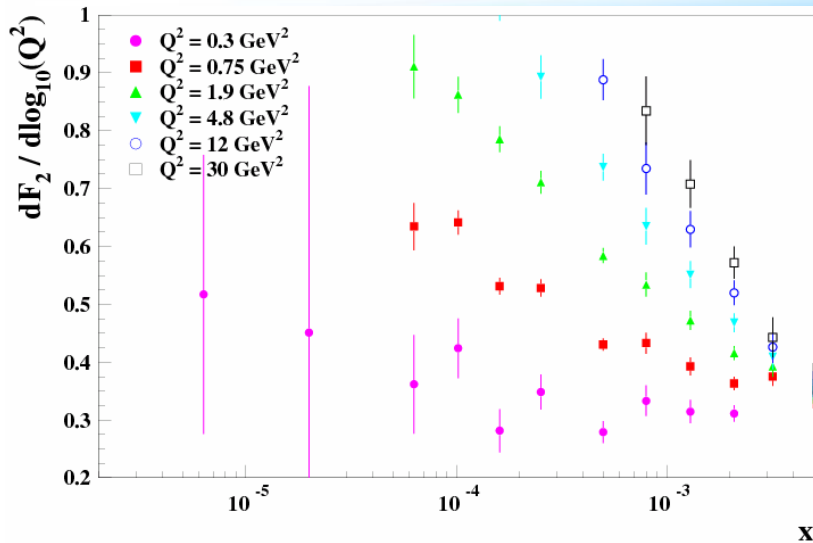
ZEUS



F_2 slopes : $dF_2/d\log_{10}(Q^2)$ at fixed x

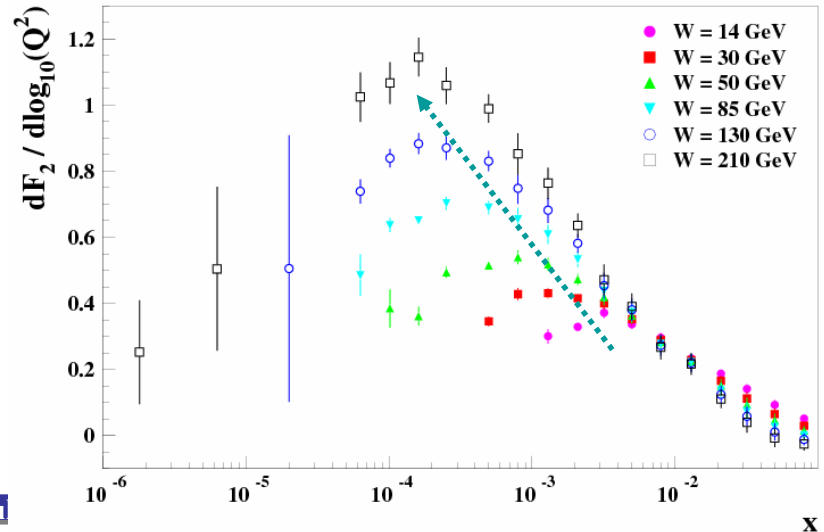
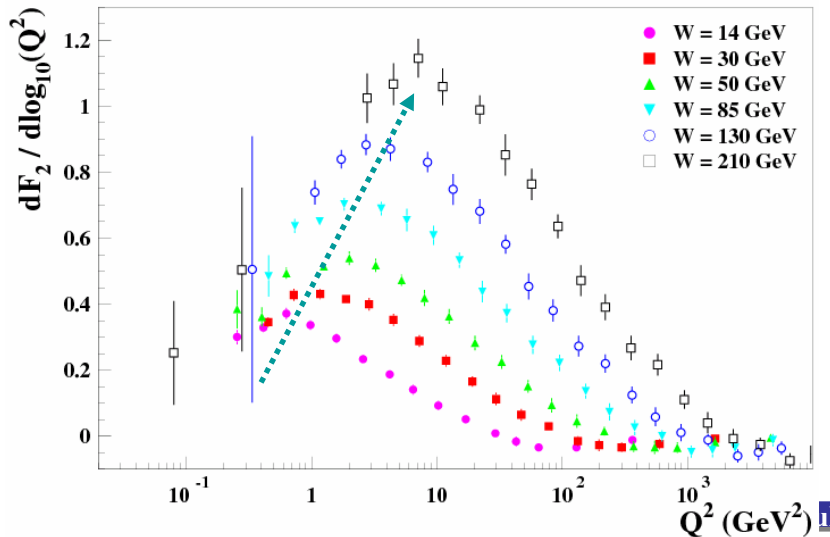
- Scaling violations are observed, which decrease as x increases.
 - Quantify it via the slope $dF_2/d\log_{10}(Q^2)$
 - Fit $F_2(x, Q^2) = A(x) + B(x)\log_{10}(Q^2) + C(x)(\log_{10}(Q^2))^2$ to the data in bins of x.
- In order to make the transition region more visible,
 - $dF_2/d\log_{10}(Q^2)$ at fixed Q^2
 - $dF_2/d\log_{10}(Q^2)$ at fixed W

$dF_2/d\log_{10}(Q^2)$



- $dF_2/d\log(Q^2)$ at fixed Q^2
The strong rise with x becomes steeper as Q^2 increases.
- $dF_2/d\log(Q^2)$ at fixed W
✓ Transition at Q^2 (or at x) is observed.

→ This observation reflects the fact that for low Q^2 , the sea quark continues to rise as $x \rightarrow 0$, whereas the rise of the gluon distribution becomes less steep or may even tend to zero.



Summary

• Diffraction in DIS

- ✓ Indication for **Regge factorisation breaking** seen in
 - Q^2 dependence of $\alpha_{\text{IP}}^{\text{diff}}(0)$
 - Q^2 dependence of $x_{\text{IP}} F_2^{\text{D}(3)}$ for fixed β and fixed x_{IP}
- ✓ Diffractive contribution of the total cross section

	$M_x < 2 \text{ GeV}$	Higher M_x
$\sigma^{\text{diff}}/\sigma^{\text{tot}}$	<i>Decreasing with W</i>	<i>Constant with W</i>
← $\alpha_{\text{IP}}^{\text{diff}}(0)$	No Q^2 dependence Soft Pomeron	Q^2 dependence Breaking of single Pomeron exchange
$\sigma^{\text{diff}}/\sigma^{\text{tot}}$	<i>Decreasing with Q^2</i>	<i>Constant with Q^2</i>
← $Q^2 \sigma^{\text{diff}}$	Higher twist behaviour	Leading twist behaviour

- ✓ Diffraction shows evidence for **pQCD evolution with Q^2 as $x_{\text{IP}} \rightarrow 0$ or $\beta \rightarrow 0$.**
- ✓ Data can be described by color dipole model (BEKW, GBW, FS04, CGC).

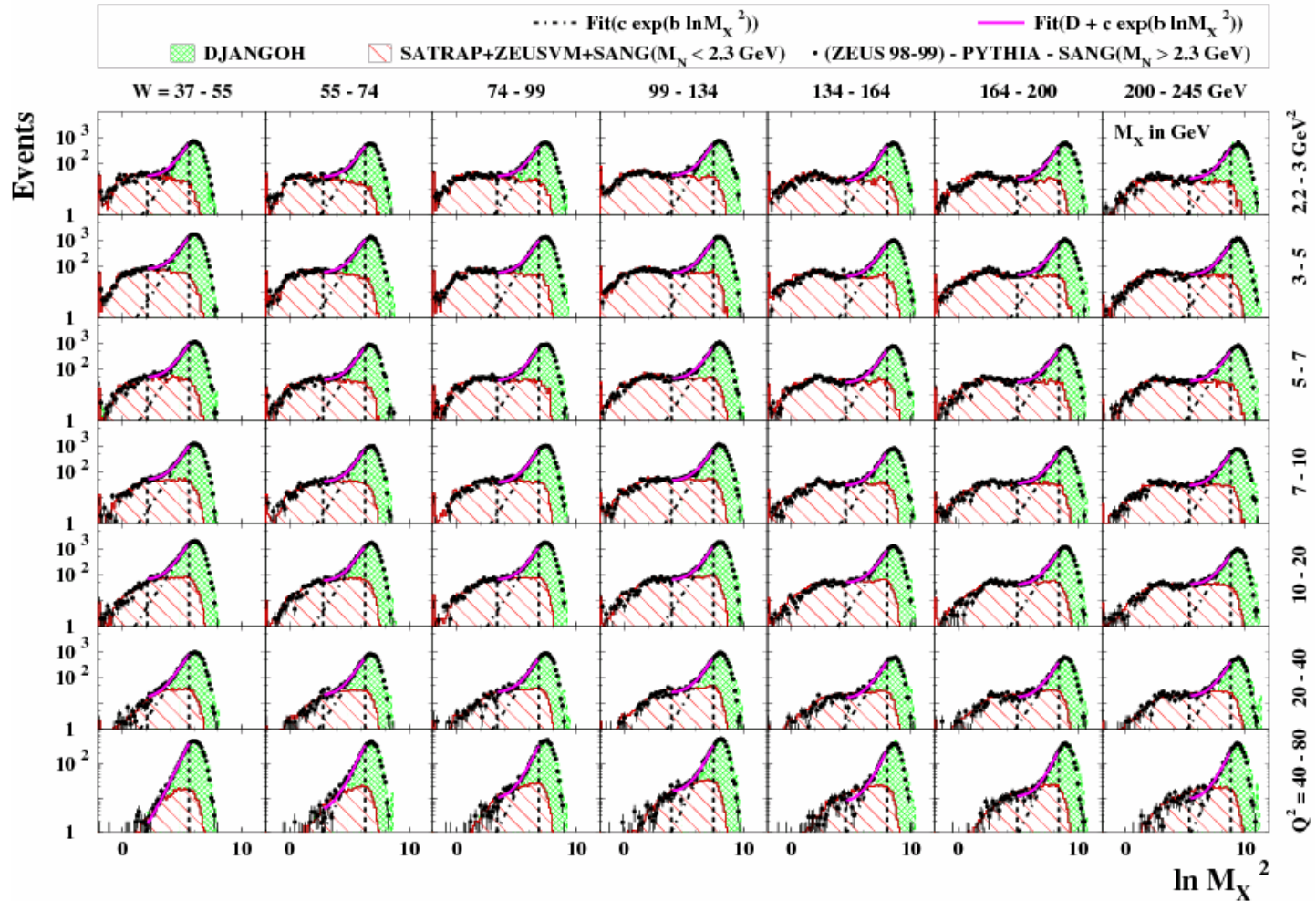
• Phenomenology of F_2

- ✓ Slopes of F_2 , $\text{dln}F_2/\text{dln}(1/x) \equiv \lambda$ and $\text{d}F_2/\text{dlog}_{10}(Q^2)$ are determined using ZEUS and the fixed target experiments.
- ✓ Study shows a clear change in the transition between photoproduction and DIS.

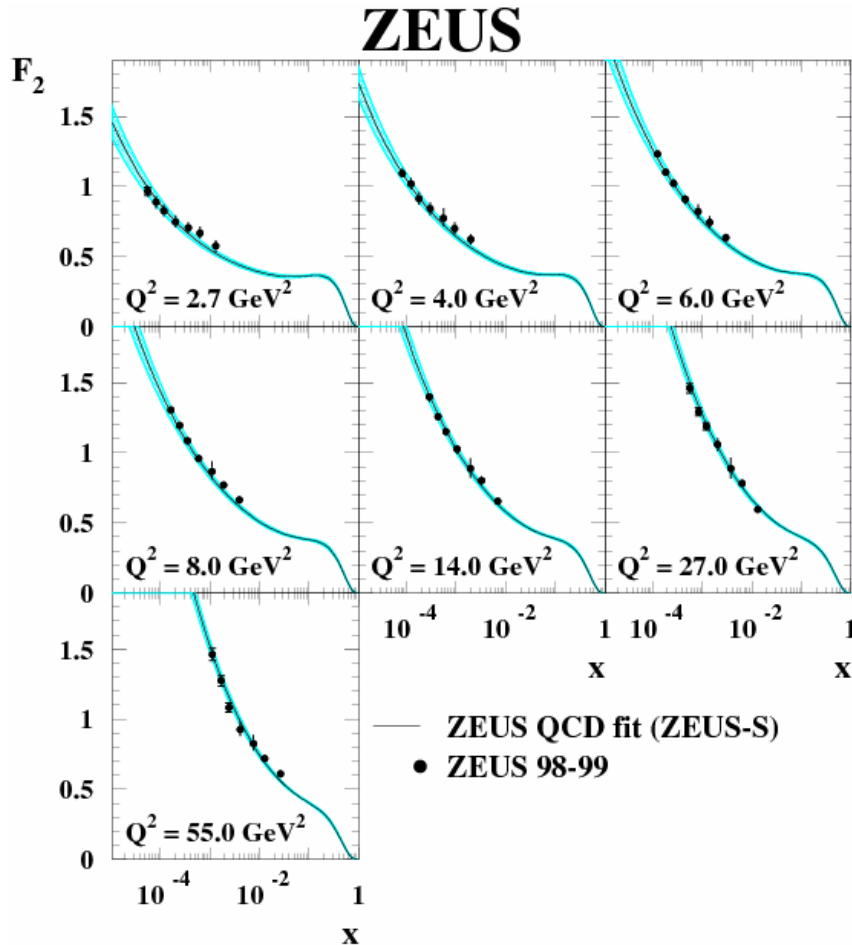
Backup Slides

Distributions of $\ln M_X^2$

ZEUS



Proton structure function, $F_2(x, Q^2)$



with $Y_{\pm} = 1 \pm (1-y)^2$

$$\frac{d^2\sigma^{e^-p}}{dx dQ^2} = \frac{2\pi\alpha^2}{xQ^4} \left[Y_+ \boxed{F_2} - y^2 F_L + Y_- xF_3 \right]$$

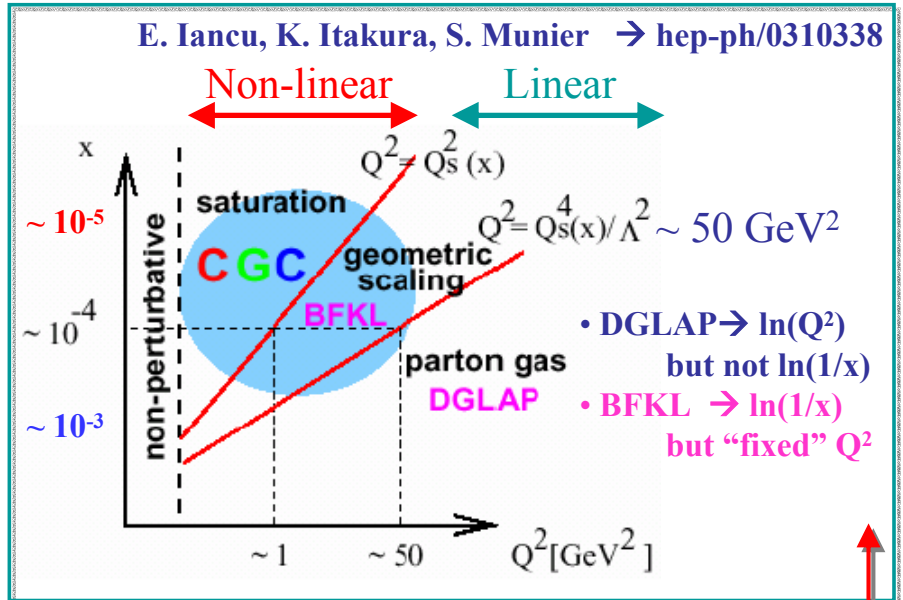
↑ Dominant contribution
↑ Sizeable only at high y
↑ Contribution important at high $Q^2 > 1000 \text{ GeV}^2$

- Good agreement with ZEUS QCD fit obtained from the previous ZEUS F_2 measurements.

Colour Glass Condensate (CGC)

Golec-Biernat, Wüsthoff, Bartels, Kowalski, Teaney, Gotsman, Levin, Lublinsky, Maor, Tuchin, McLerran, Mueller, Iancu, Itakura, Munier

- **Colour :**
gluons have “colour” in QCD.
- **Glass :**
the fields evolve very slowly with respect to the natural time scale and are disordered.
- **Condensate :**
It's a dense matter of gluons
→ Very high density $\sim 1/\alpha_s$.
Interactions prevent more gluon occupation.



Develop Golec-Biernat, Wüsthoff model :

$$\sigma_{\text{dipole}}(x, r_{\perp}) = \sigma_0 \left[1 - \exp \left\{ -\frac{1}{4} r_{\perp}^2 Q_s^2(x) \right\} \right]$$

✓ Saturation : $\sigma_{\text{dipole}} \rightarrow \sigma_0$ as $r_{\perp} \rightarrow \infty$

✓ Good fit to the old HERA data for $x < 10^{-2}$.

But, doesn't work for new HERA data at high Q^2 .

$$Q_s^2(x) = 1 \text{ GeV}^2 (x_0/x)^{\lambda}$$

→ Adding DGLAP evol. at high Q^2 (small r_{\perp}) → Saturation for $Q^2 < Q_s^2(x)$

→ Adding impact parameter, b dependence → BFKL dynamics in $Q^2 < Q_s^4(x)/\Lambda^2$

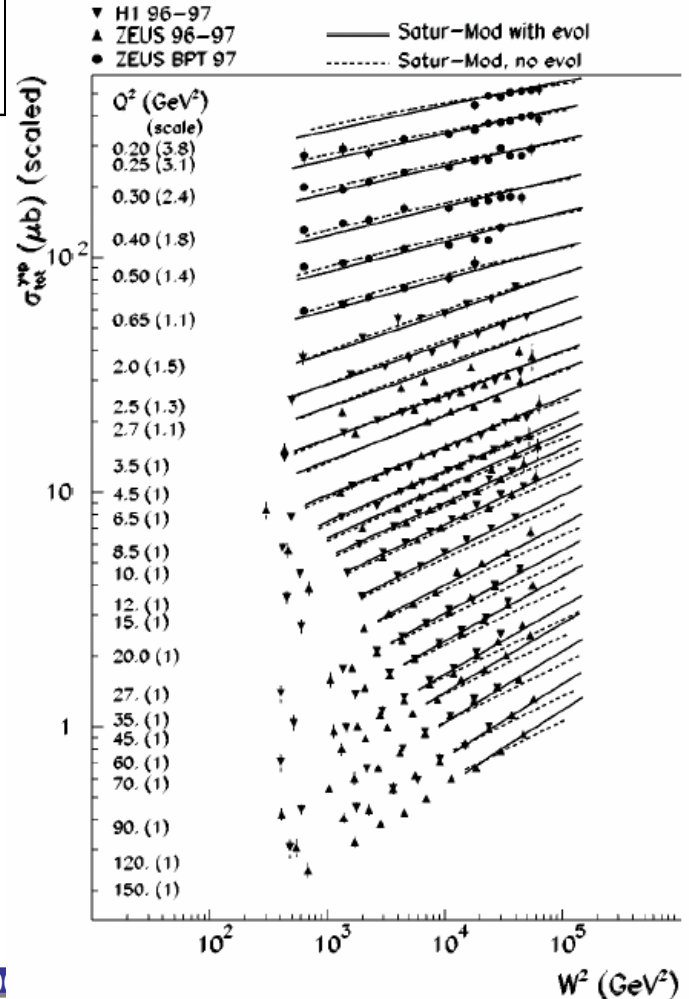
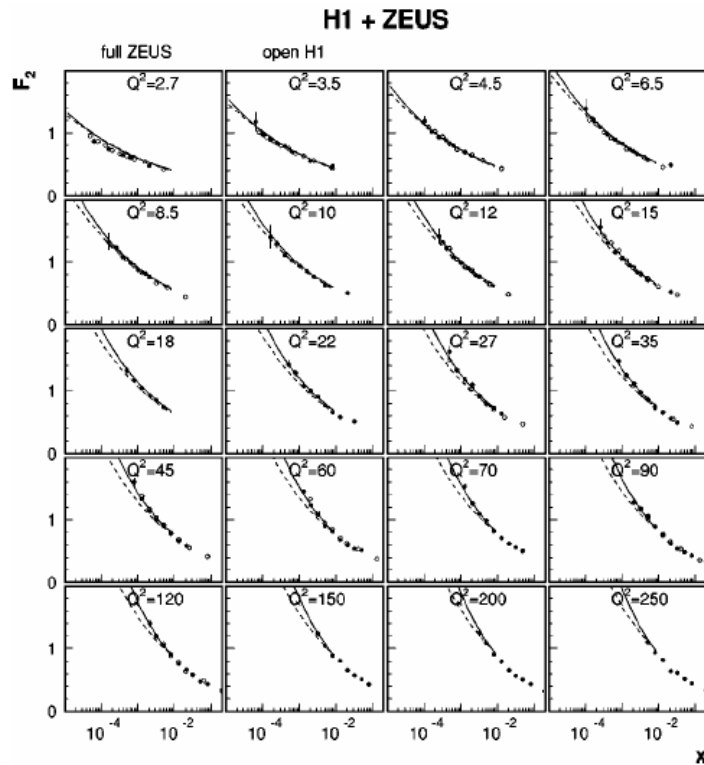
CGC II – Saturation model with DGLAP

Bartels, Golec-Biernat, Kowalski

→ PRD66(02)014001

By adding DGALP evolution at high Q² (small r_⊥)

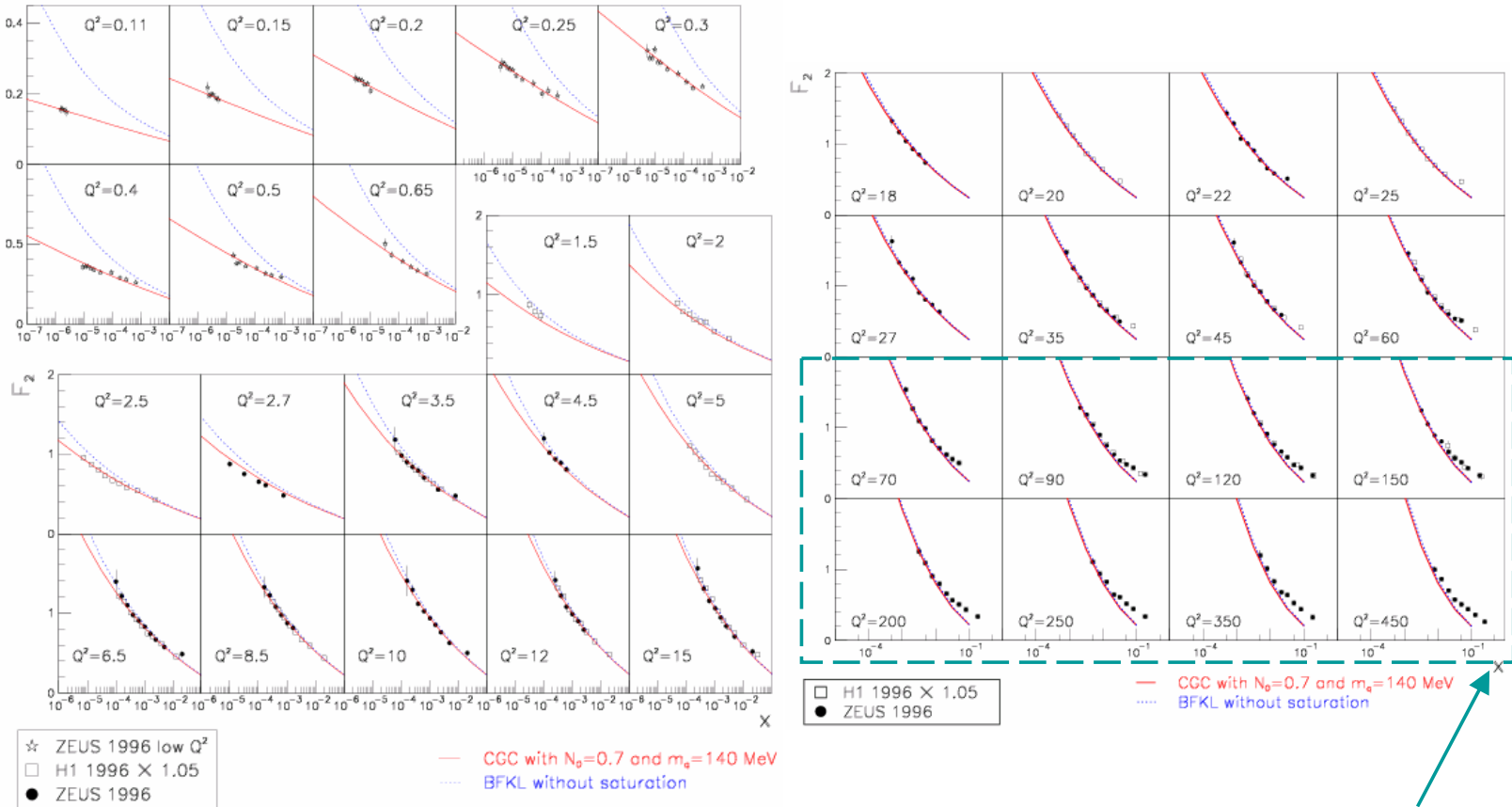
$$\sigma_{\text{dipole}}(x, r_{\perp}) = \sigma_0 \left[1 - \exp \left\{ - \frac{\pi^2 \alpha_S(\mu^2)}{3\sigma_0} r_{\perp}^2 x G(x, \mu^2) \right\} \right]$$



CGC III-Saturation and BFKL

Iancu, Itakura, Munier

→ hep-ph/0310338



DGLAP regime

Diffractive hard scattering factorisation

[Collins (1998); Trentadue, Veneziano (1994); Berera, Soper (1996)...]

$$\sigma^D(\gamma^* p \rightarrow Xp) = \underbrace{f_{i/p}^D(z, Q^2, x_{IP}, t)}_{\text{Diffractive parton distribution function}} \otimes \underbrace{\hat{\sigma}_{\gamma^* i}^D(z, Q^2)}_{\text{Universal partonic cross section}}$$

Diffractive parton distribution function **Universal partonic cross section**

$f_{i/p}^D(z, Q^2, x_{IP}, t)$: Probability to find in a proton, with a probe of resolution Q^2 , parton i with momentum fraction z , under the condition that the proton remains intact and emerges with small energy loss, x_{IP} , and momentum transfer, t .

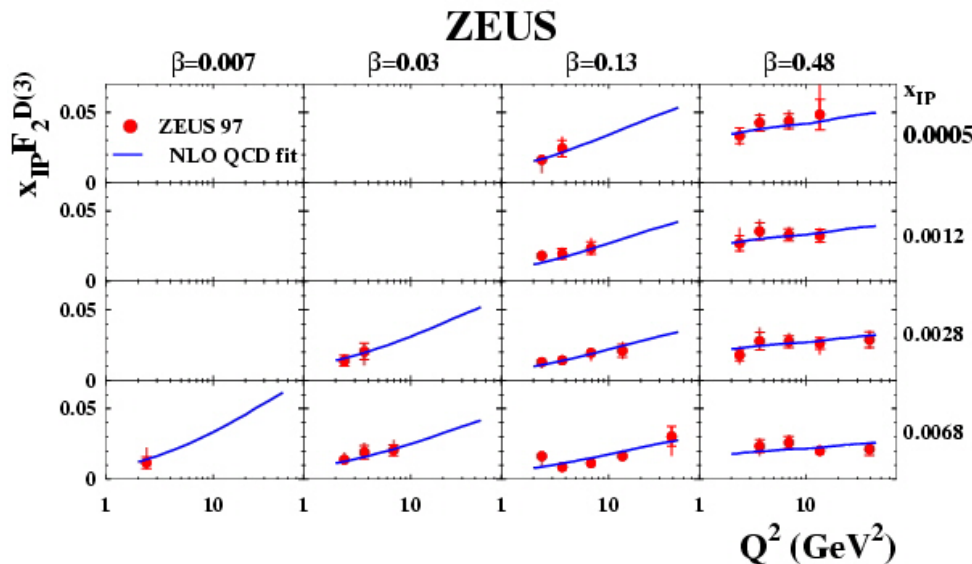
ZEUS NLO QCD fits

- Perform fit to the results of $x_{IP} F_2^{D(3)}$ with $x_{IP} < 0.01$ and $Q^2 > 2 \text{ GeV}^2$
- Assume the Regge factorisation using Donnachie and Landshoff Pomeron flux

$$F_2^{D(3)}(\beta, Q^2, x_{IP}) = f_{IP}(x_{IP}) \cdot F_2^{IP}(\beta, Q^2) \quad f_{IP}(x_{IP}) \propto \int \frac{e^{b_0^{IP} t}}{x_{IP}^{2\alpha_{IP}(t)-1}} dt$$

- Parametrise PDFs (quark flavour singlet and gluon) using $zf(z) = (a_1 + a_2 z + a_3 z^2)(1-z)^{a_4}$
 - ✓ For light quark distribution, assuming $u = d = s = \bar{u} = \bar{d} = \bar{s}$
 - ✓ Charm quarks were treated in Thorne-Roberts variable flavor number (TRVFN) scheme with $m_c = 1.45 \text{ GeV}$.
- NLO evolution : QCDNUM

NLO QCD fit on LPS+charm data

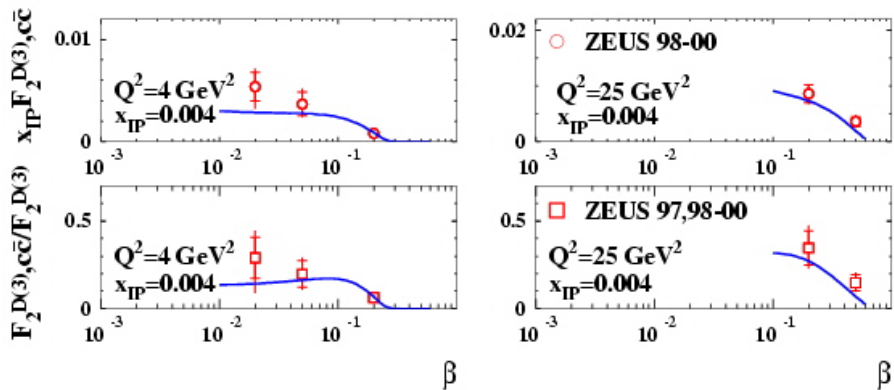


- QCD fit describes data with $\chi^2/\text{ndf} = 37.8/36$

- Fraction of the t-channel momentum carried by gluons

ZEUS at $Q^2=2 \text{ GeV}^2$

$$82 \pm 8(\text{stat.})_{-16}^{+5} (\text{syst.})\%$$



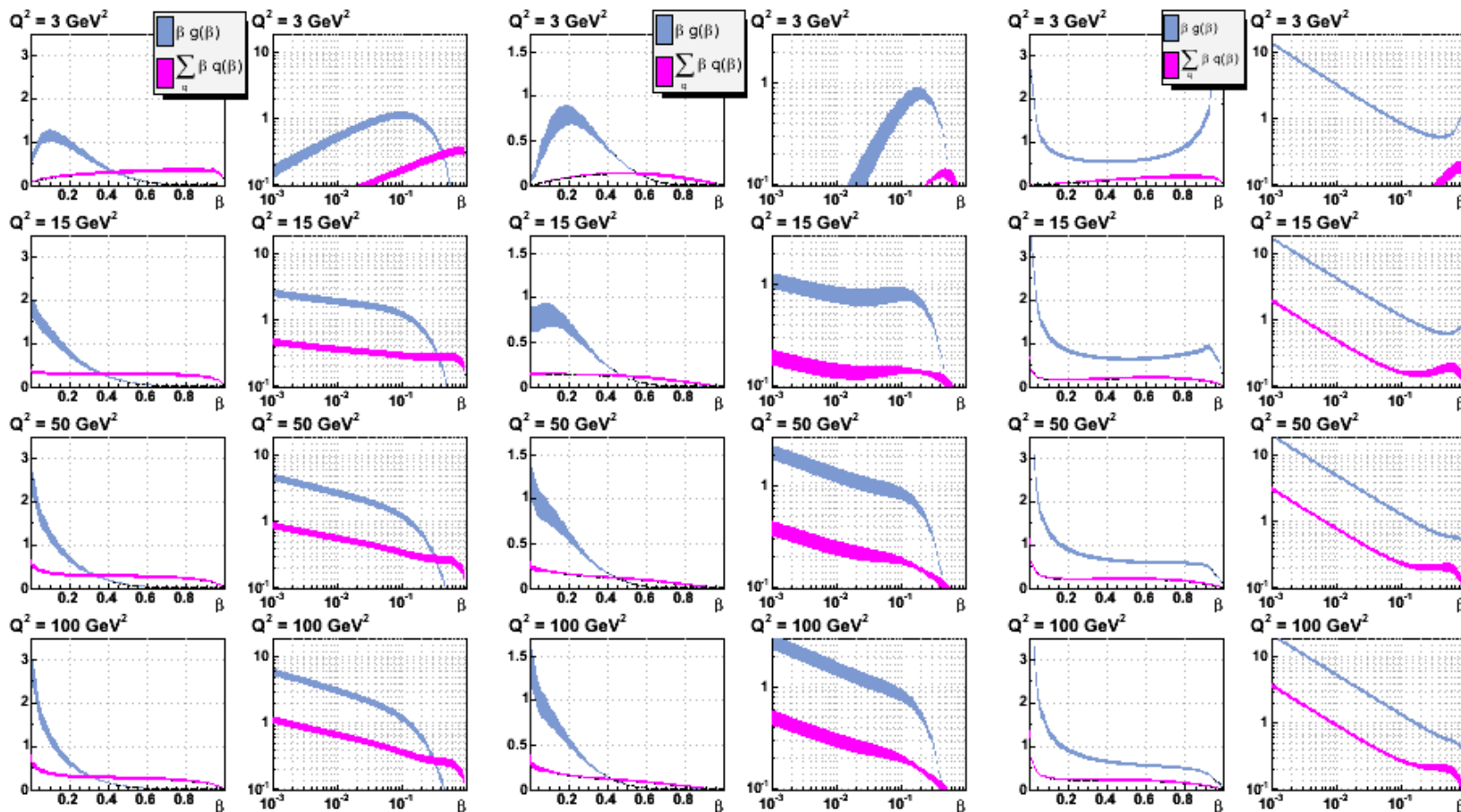
Diffractive parton distribution functions (DPDF)

DIS05, A. Levy.

ZEUS FPC

ZEUS LPS

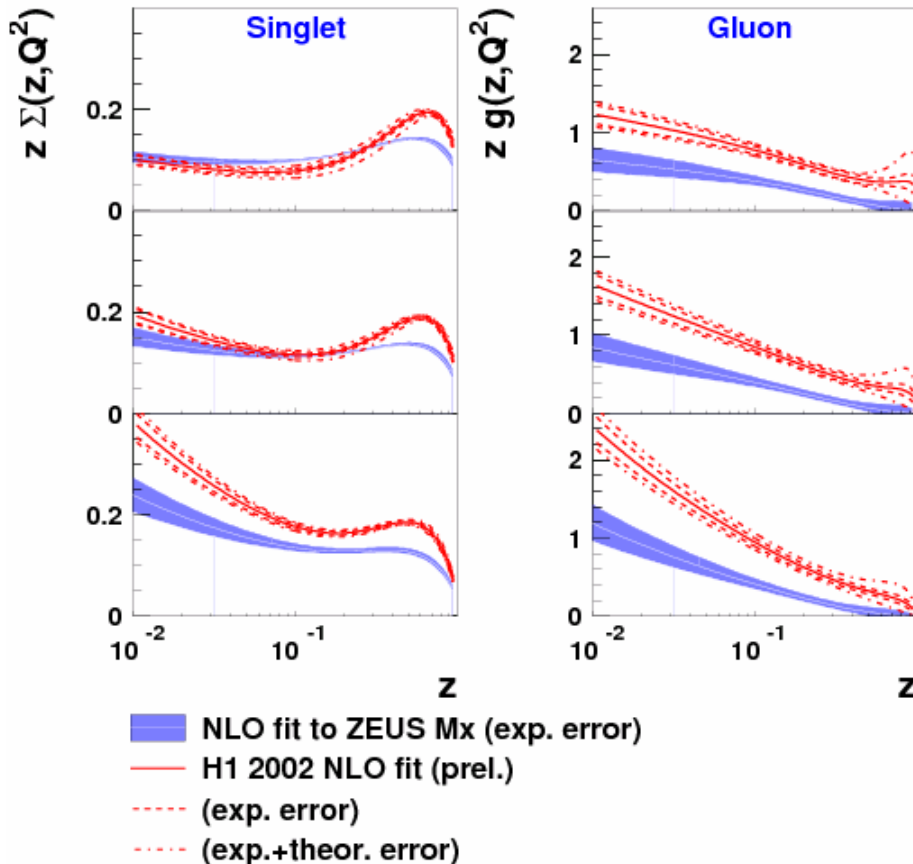
H1



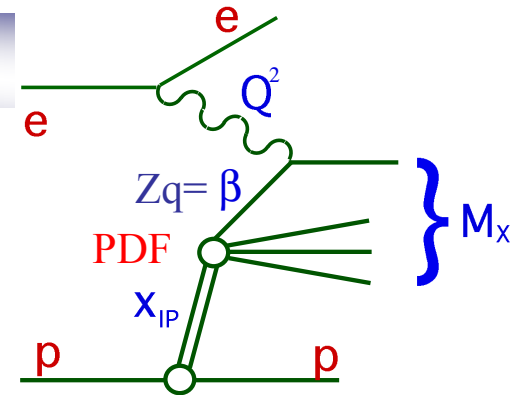
H1 NLO QCD fit to ZEUS M_X data

P. Newman and P. Schilling

NLO QCD fits to H1 and ZEUS data



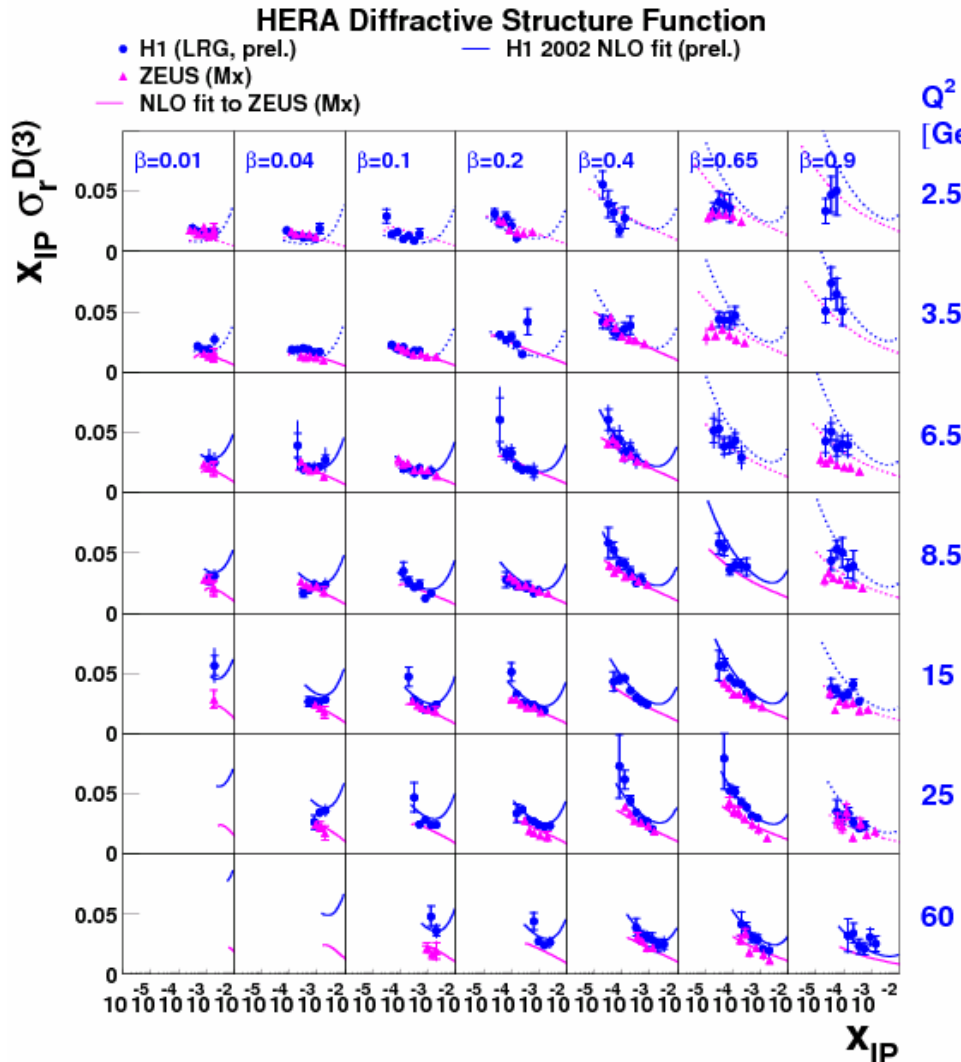
Q^2
 [GeV²]
 6.5



- Perform the H1 2002 NLO fit to ZEUS M_X data.
- 15 • ZEUS M_X data scaled to $M_N < 1.6$ GeV
- No Reggeon contribution needed.
- 90 • Singlet similar at low Q^2 , evolving differently to higher Q^2 due to coupling to gluon.
- Significant difference between diffractive gluon densities from H1 and ZEUS M_X .

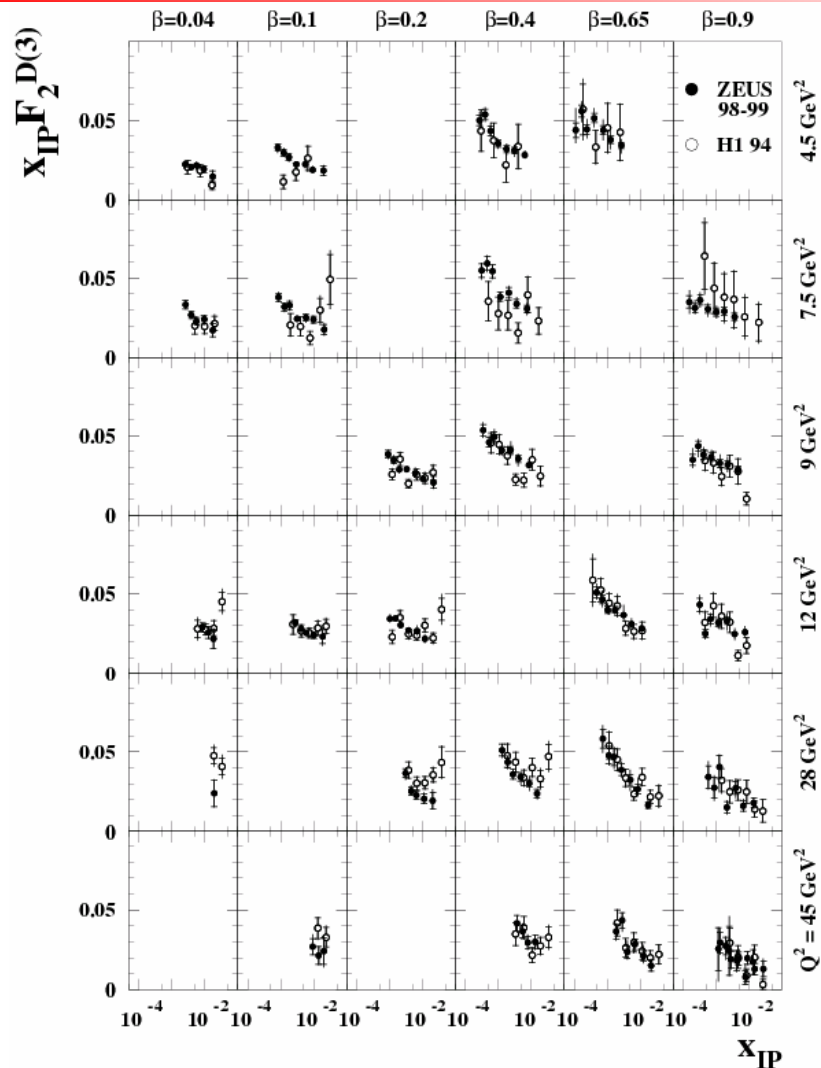
Comparison H1 LRG with ZEUS M_X data

P. Newman and P. Schilling



- Reggeon contribution in H1 LRG data.
- Difference in data at high β (low M_X) region.
- Smaller positive scaling violation in ZEUS M_X data
 → Leading to smaller gluon

Comparison H1 LRG (94) with ZEUS M_x data



MRW (Martin, Ryskin, Watt) fit - I

$$F_2^{D(3)} = \sum_{a=q,g} C_{2,a} \otimes a^D$$

EPJC 37 (2004) 285,
HERA-LHC workshop .

Thanks to G. Watt!

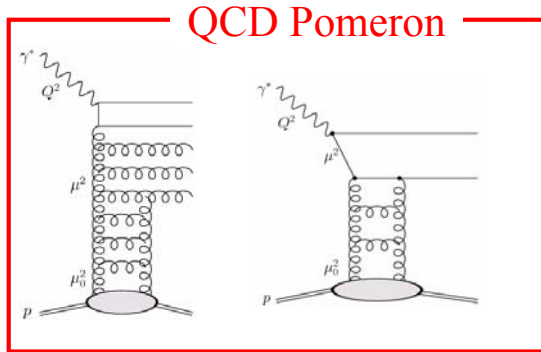
Diffractive PDFs $a^D = zq^D$ or zg^D

$$F_2^{D(3)} = F_{2,pert.}^{D(3)} + F_{L,tw.4}^{D(3)} + F_{2,direct}^{D(3),c\bar{c}} + F_{2,non-pert.}^{D(3)} + F_{2,IR}^{D(3)}$$

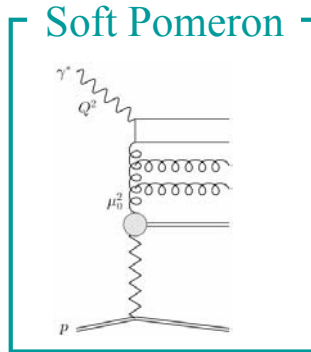
1998/99 ZEUS M_x data

"pQCD" fit (all contributions)

--- Perturbative contrib.
--- Non-perturbative contrib.
--- Twist-4 contrib.
--- 'Direct' charm contrib.



QCD Pomeron



Soft Pomeron

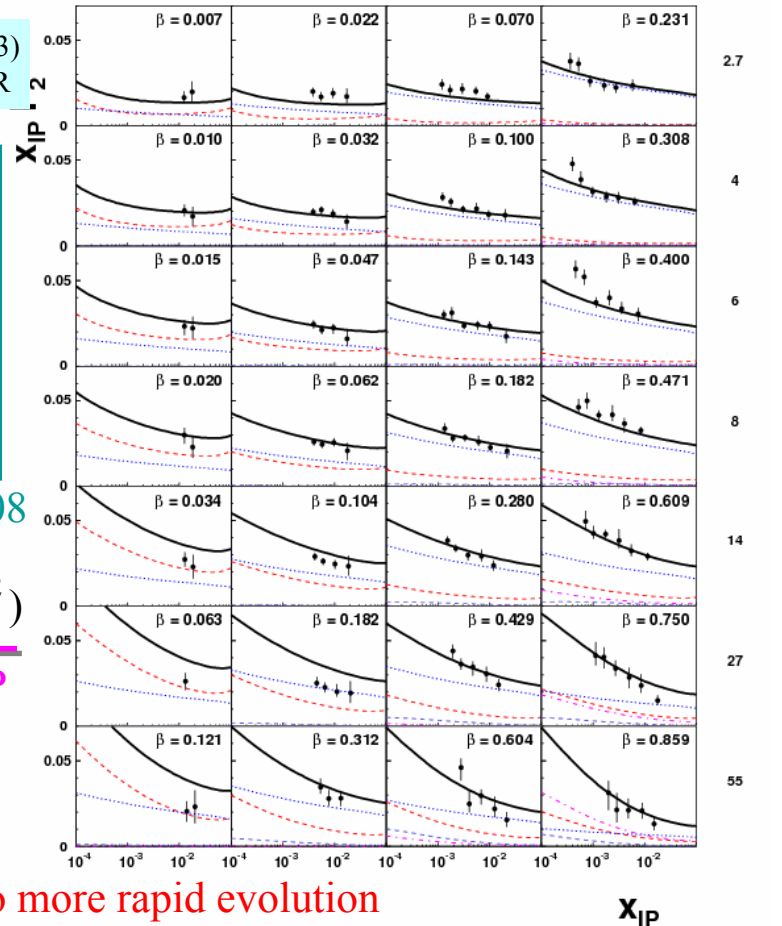
Regge factorisation with $\alpha_{IP}^{soft}(0) = 1.08$

$$a_{pert.}^D(x_{IP}, z, Q^2) = \int_{\mu_0^2}^{Q^2} \frac{d\mu^2}{\mu^2} f_{IP}(x_{IP}; \mu^2) a^{IP}(z, Q^2; \mu^2)$$

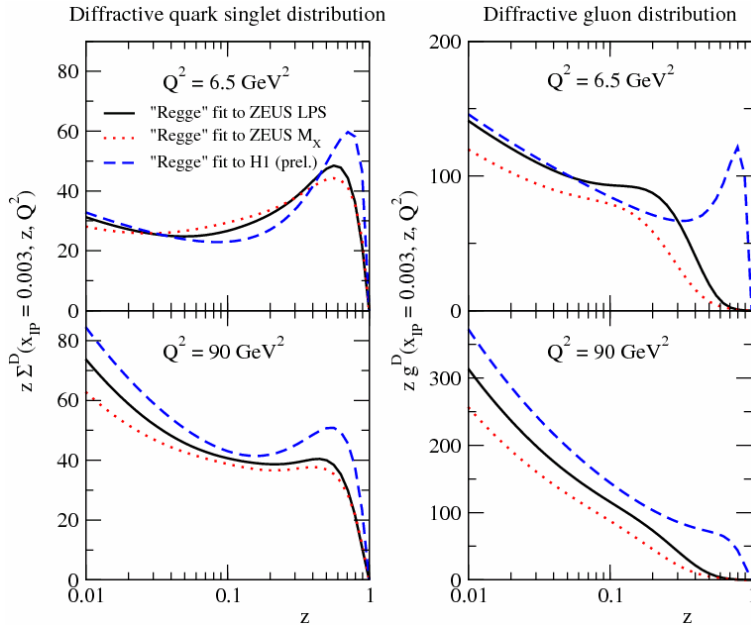
Evolving using NLO DGLAP

$$\frac{\partial a^D}{\partial \ln Q^2} = \frac{\alpha_S}{2\pi} \sum_{a'=q,g} P_{aa'} \otimes a'^D + P_{aIP}(z) f_{IP}(x_{IP}; Q^2)$$

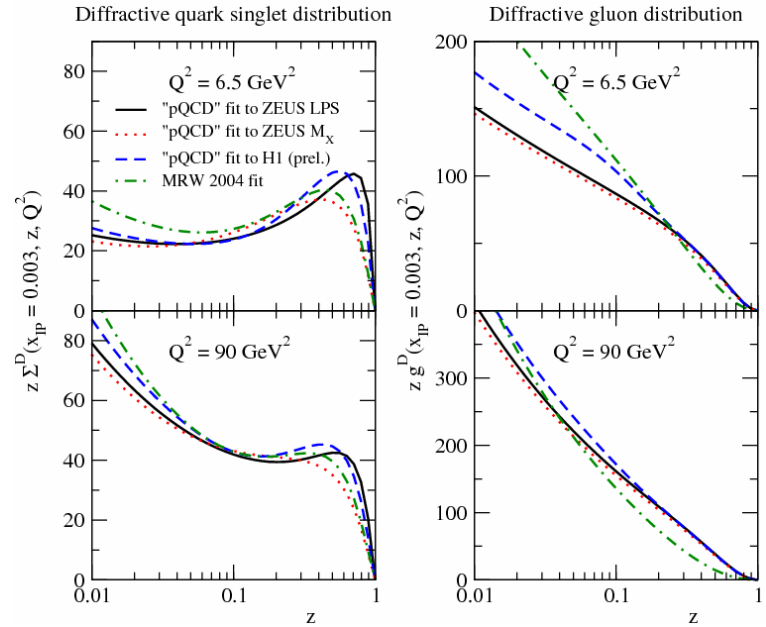
Extra inhomogeneous term \rightarrow leading to more rapid evolution



“Regge” approach



“pQCD” approach



➔ Similar way like the H1 NLO QCD fit.

- Different shapes comparing with the parton distributions from H1/ZEUS NLO QCD fit.

➔ QCD Pomeron + Soft Pomeron

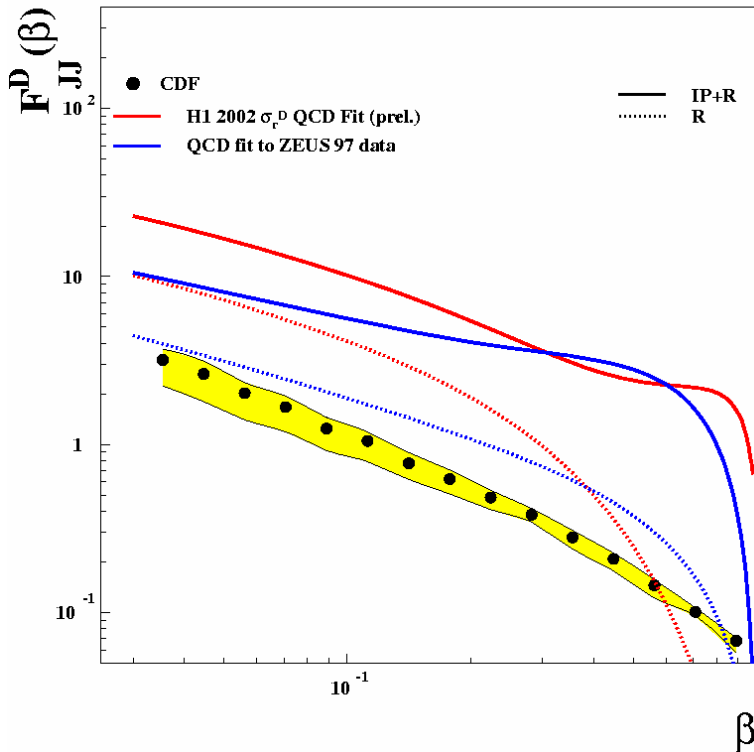
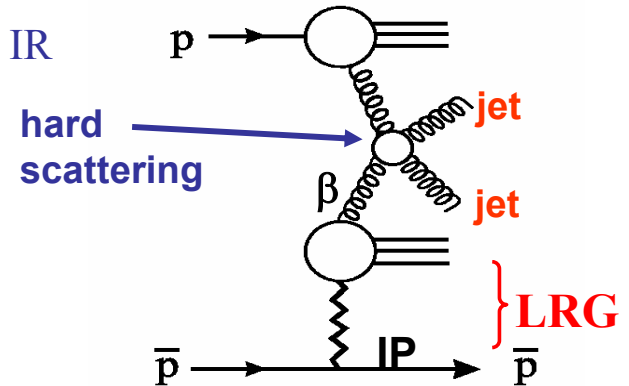
- Parton distributions from ZEUS LPS, ZEUS M_X , and H1 are similar.

DPDFS are affected by the initial conditions, assumptions and models.

➔ The reason of “ $g^D(\text{H1}) > g^D(\text{ZEUS } M_X)$ ” might be related to “theory used”.

CDF data vs H1 / ZEUS PDFs

$$F_{JJ}^D(\beta) = \beta \left[g(\beta) + \frac{4}{9} q(\beta) \right] \quad \text{from diffractive PDF and IR}$$



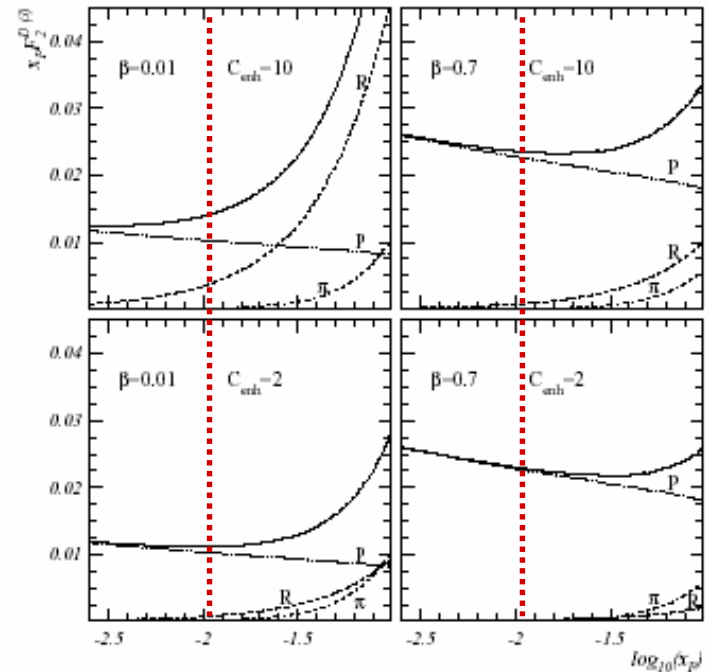
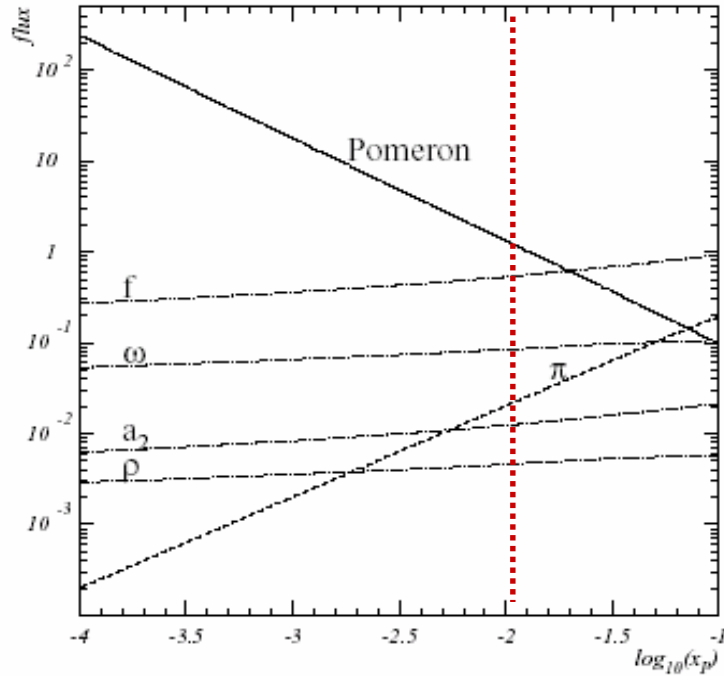
- Compare data with QCD predictions based on PDFs extracted from NLO DGLAP fits
 → QCD factorization breaks in $p\bar{p}$ hard scattering.

→ Rapidity gap ‘survival probability’ due to multi-Pomeron exchange in $p\bar{p}$

(Kaidalov, Khoze, Martin, Ryskin)

Reggeon and pion contributions in diffraction

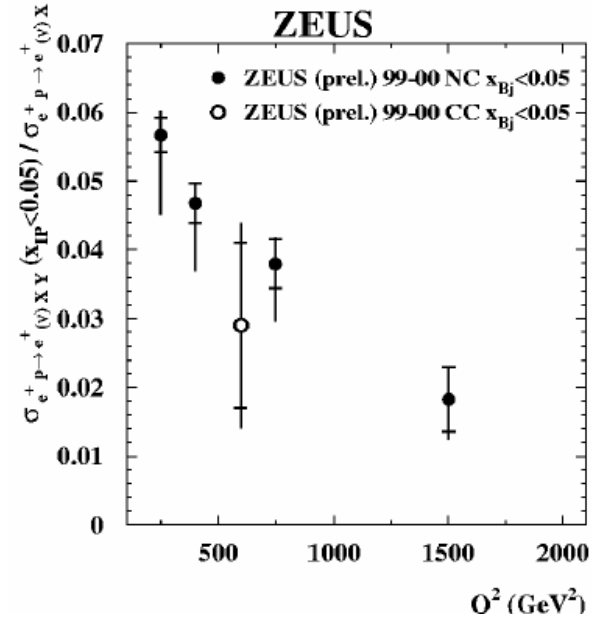
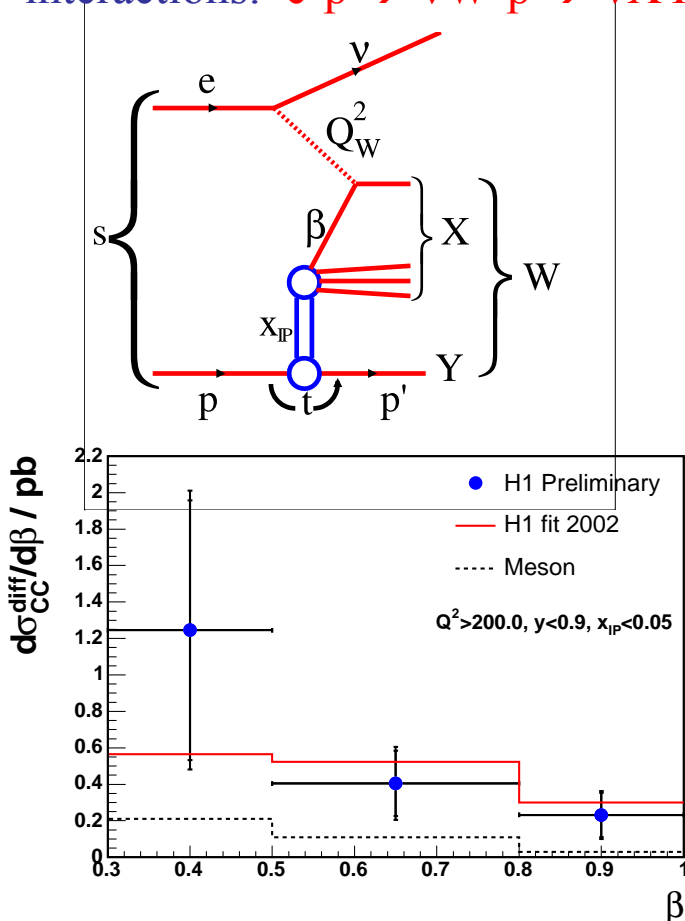
K. Golec-Biernat, J. Kwiecinski and A. Szczurek, Phys. Rev. **D56** (1997) 3955.



DIS05, A. Levy.

High Q^2 charged current diffractive events

Probe diffractive process via weak interactions: $e^+p \rightarrow \nu W^+p \rightarrow \nu XY$



Ratio of LRG to inclusive CC cross section :

$$\text{ZEUS} : \sigma_{\text{LRG}}^{\text{CC}} / \sigma_{\text{inc}}^{\text{CC}} = 2.9 \pm 1.2(\text{stat.}) \pm 0.8(\text{sys.})\%$$

$$\text{H1} : \sigma_{\text{LRG}}^{\text{CC}} / \sigma_{\text{inc}}^{\text{CC}} = 2.5 \pm 0.8(\text{stat.}) \pm 0.6(\text{sys.})\%$$

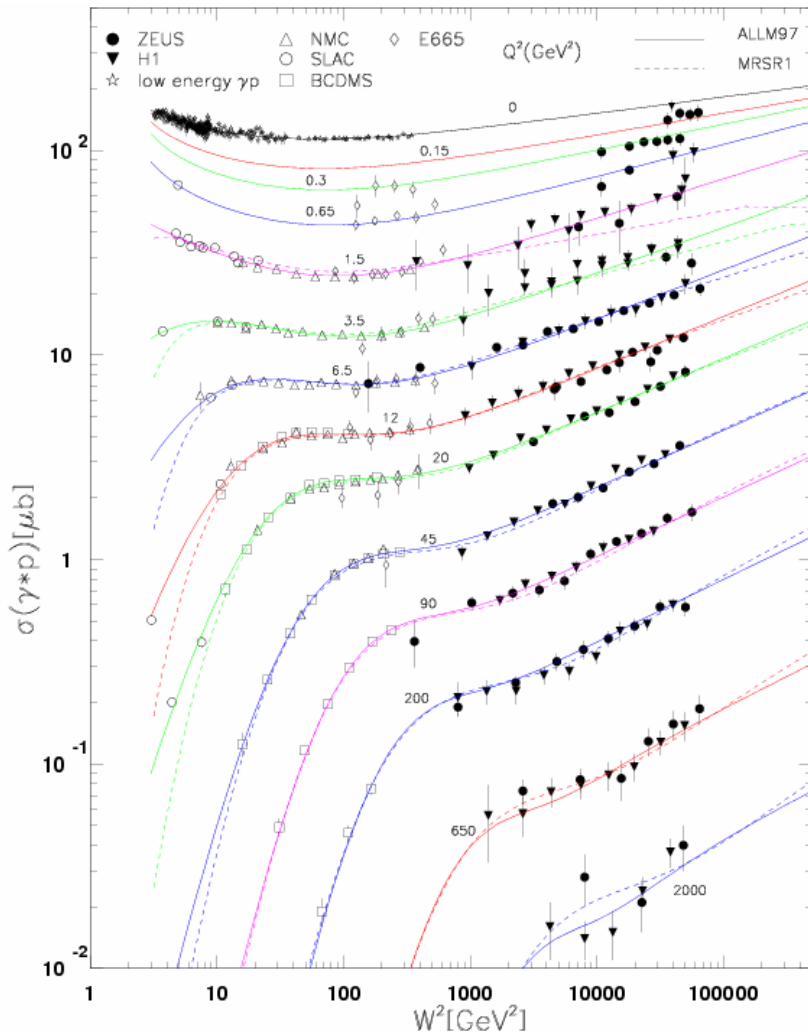
→ Results are in good agreement.

→ Diffractive PDFs from H1 LO QCD fit describe LRG CC cross sections.

ALLM97 parametrisation

Abramowicz and Levy

→ hep-ph/9712415



$$F_2(x, Q^2) = \frac{Q^2}{Q^2 + M_0^2} (F_2^{\text{IP}}(x, Q^2) + F_2^{\text{IR}}(x, Q^2))$$

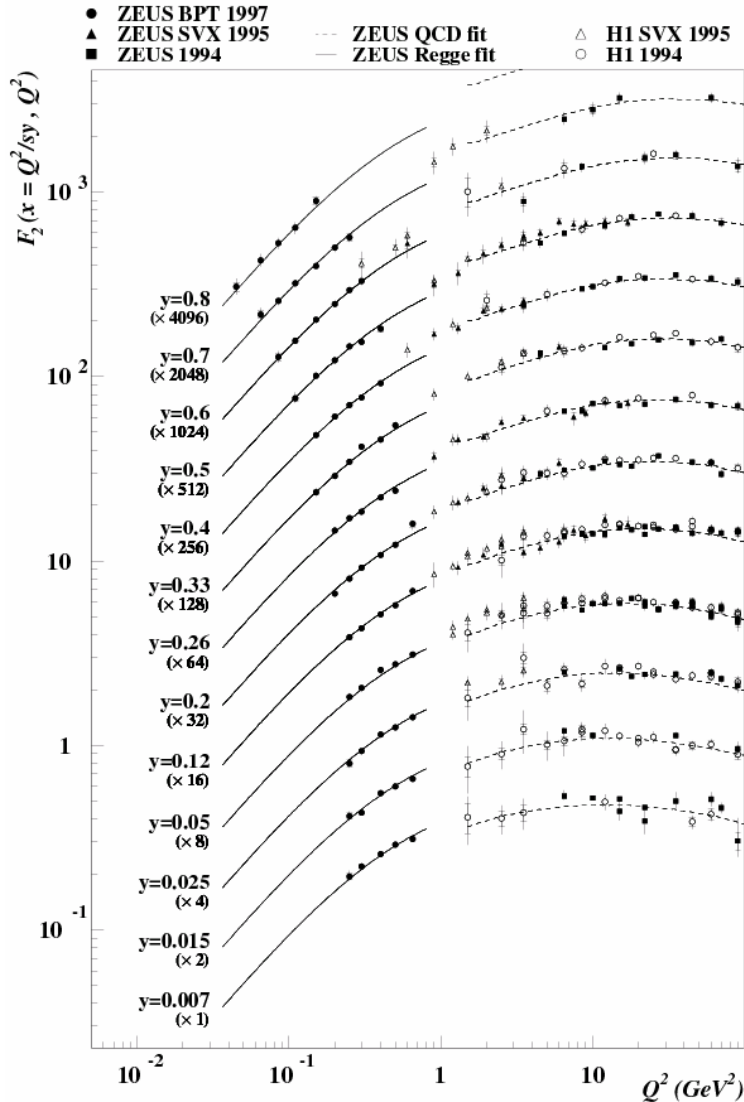
$$F_2^{\text{IP}}(x, Q^2) = c_{\text{IP}}(t) x_{\text{IP}}^{\alpha_{\text{IP}}(t)} (1-x)^{b_{\text{IP}}(t)}$$

$$F_2^{\text{IR}}(x, Q^2) = c_{\text{IR}}(t) x_{\text{IR}}^{\alpha_{\text{IR}}(t)} (1-x)^{b_{\text{IR}}(t)}$$

$$t = \ln \left(\frac{\ln \frac{Q^2 + Q_0^2}{\Lambda^2}}{\ln \frac{Q^2}{\Lambda^2}} \right), \quad \frac{1}{x_{\text{IP,IR}}} = 1 + \frac{W^2 - M^2}{Q^2 + M_{\text{IP,IR}}^2}$$

- Regge motivated approach
- 23 free parameters were determined from a fit to the data.
 - HERA 94-95 data
 - SLAC, BCDMS, E665, NMC
- $\chi^2/\text{ndf} = 0.98$

ZEUS 1997



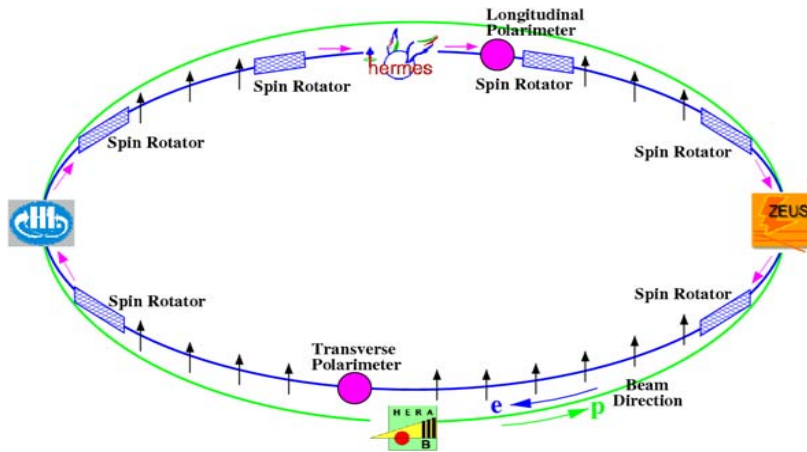
ZEUS Regge 97

ZEUS Coll. → Phys. Lett. B 487, 53 (2000)

$$F_2(x, Q^2) = \frac{Q^2}{4\pi^2 \alpha} \cdot \frac{M_0^2}{M_0^2 + Q^2} \cdot \left(A_{IR} \left(\frac{Q^2}{x} \right)^{\alpha_{IR} - 1} + A_{IP} \left(\frac{Q^2}{x} \right)^{\alpha_{IP} - 1} \right)$$

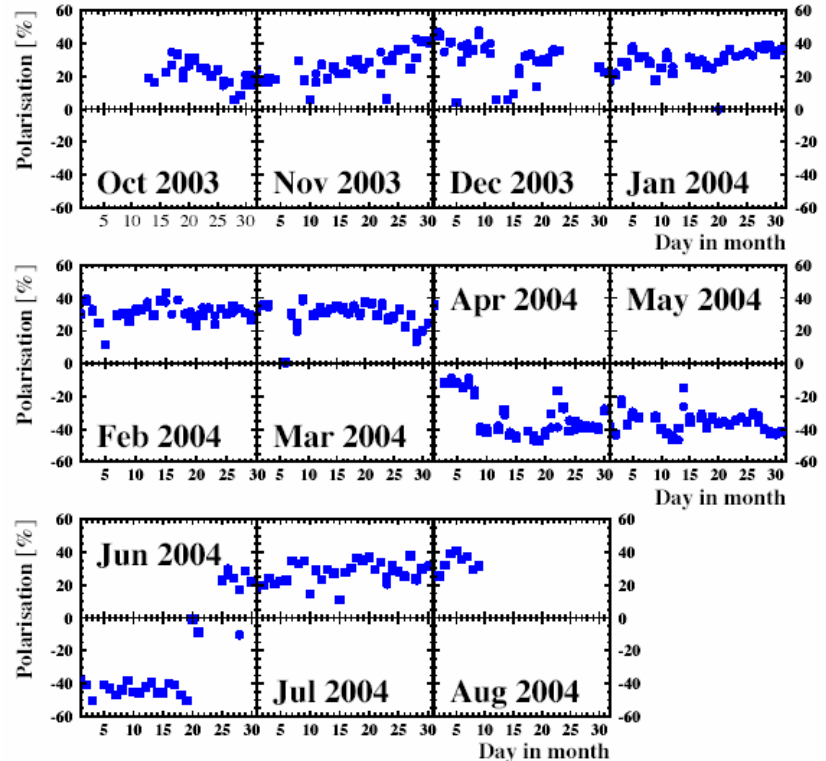
- Based on the combination of
 1. a simplified version of the generalized vector meson dominance model for the description of the Q^2 dependence.
 2. Regge theory for the description of the x dependence of F_2 .
- Fit to F_2 (ZEUS BPT 1997 with $0.04 < Q^2 < 0.74 \text{ GeV}^2$, $5.3 \cdot 10^{-7} < x < 1.6 \cdot 10^{-3}$)
 → $A_{IR}, \alpha_{IR}, A_{IP}, \alpha_{IP}, M_0$

HERA-II (2003-2007) - polarisation



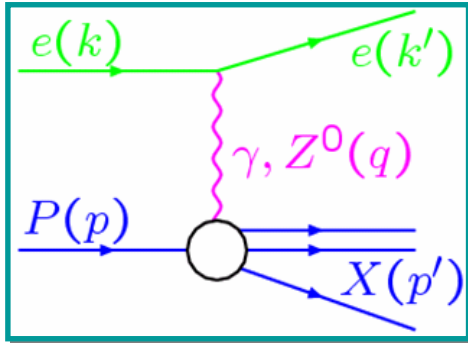
- Transverse polarisation of leptons builds up naturally.
- Spin rotators convert to longitudinal polarisation
- Measured by two independent Compton polarimeters.
- Luminosity weighted average polarisations of -40 % and +32 %.

Average HERA polarisation



Neutral current DIS cross section

NC : $e^\pm + p \rightarrow e^\pm + X$



NC Reduced cross section: $\tilde{\sigma}_{NC}(x, Q^2)$

$$\frac{d^2 \sigma^{NC}(e^\pm p)}{dx dQ^2} = \frac{2\pi \alpha^2}{x Q^4} Y_\pm \left[F_2 - \frac{y^2}{Y_+} F_L \mp \frac{Y_-}{Y_+} x F_3 \right] \quad Y_\pm = 1 \pm (1-y)^2$$

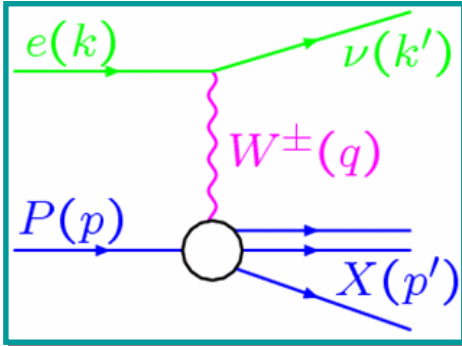
↑ Dominant contribution
↑ Sizeable only at high y
↑ Contribution only important at high Q^2

$$F_2 = F_2^{em} + \frac{Q^2}{Q^2 + M_Z^2} F_2^{\gamma Z} + \left[\frac{Q^2}{Q^2 + M_Z^2} \right]^2 F_2^Z \propto \sum_{q=u\dots b} (q + \bar{q})$$

$$xF_3 = \frac{Q^2}{Q^2 + M_Z^2} xF_3^{\gamma Z} + \left[\frac{Q^2}{Q^2 + M_Z^2} \right]^2 xF_3^Z \propto \sum_{q=u\dots b} (q - \bar{q})$$

Charged current DIS cross section

$$\text{CC} : e^\pm + p \rightarrow \bar{\nu}_e (\nu_e) + X$$



cross section:

$$\frac{d^2\sigma^{CC}(e^+p)}{dx dQ^2} = \frac{G_F^2}{4\pi x} \left(\frac{M_W^2}{M_W^2 + Q^2} \right)^2 \left[\bar{u} + \bar{c} + (1-y)^2(d+s) \right]$$

CC e⁻p cross section:

$$\frac{d^2\sigma^{CC}(e^-p)}{dx dQ^2} = \frac{G_F^2}{4\pi x} \left(\frac{M_W^2}{M_W^2 + Q^2} \right)^2 \left[u + c + (1-y)^2(\bar{d} + \bar{s}) \right]$$

Electron/positron-proton collisions probe different quark content of proton

Big difference in cross section magnitude

Cross sections suppressed due to large mass of W boson compared to NC DIS

Polarised DIS cross sections

NC cross section modified by P:

$$\frac{d^2\sigma(e^\pm p)}{dx dQ^2} = \frac{2\pi\alpha^2}{xQ^4} \left[H_0^\pm + PH_P^\pm \right] \quad P = \frac{N_R - N_L}{N_R + N_L}$$

Unpolarised contribution

Polarised contribution - only includes Z and γZ terms

Polarised contribution only significant at high Q^2 - **subtle effect at HERA**

CC cross section modified by P:

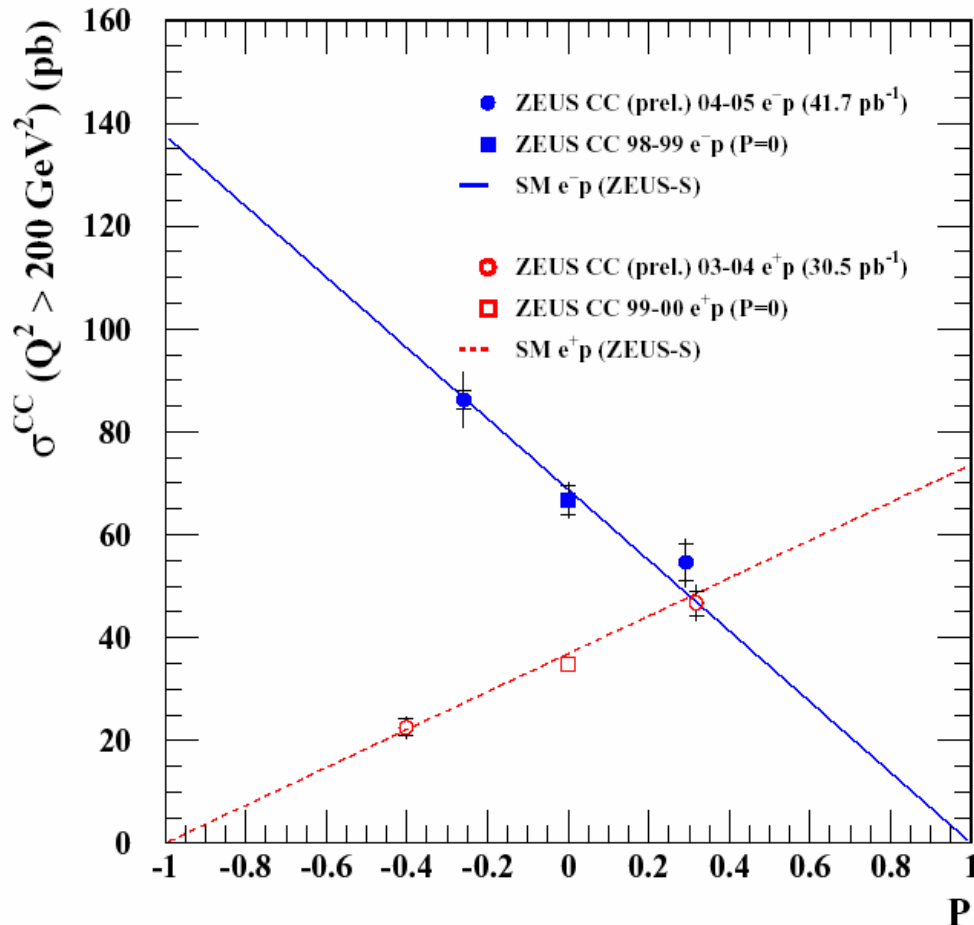
$$\sigma_{CC}^{e^\pm p}(P) = (1 \pm P) \cdot \sigma_{CC}^{e^\pm p}(0)$$

Polarisation scales P=0 cross section linearly - **clear and large effect at HERA**

This page could be merged with the next two page!

Spin-dependent CC cross section

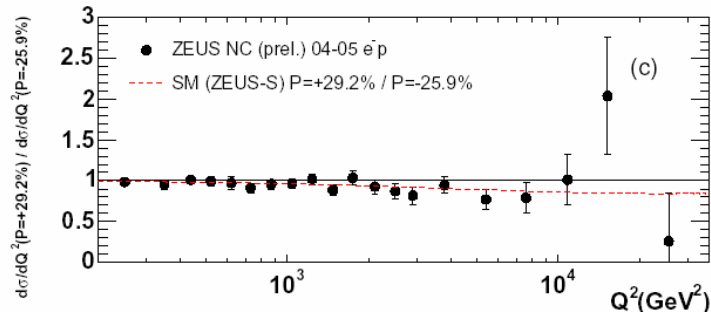
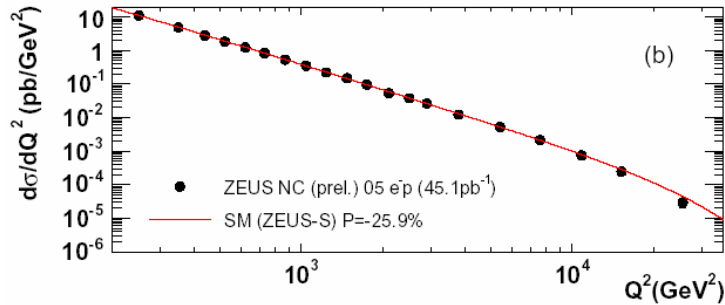
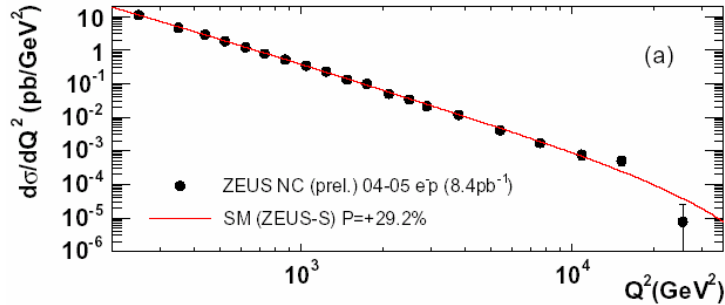
ZEUS



- For e^-p scattering,
No hint of RH CC $\sigma(P=-1) = 0$
- For e^+p scattering,
No hint of RH CC $\sigma(P=+1) = 0$
- Can test spin-dependent part of SM.

Spin-dependent NC cross section

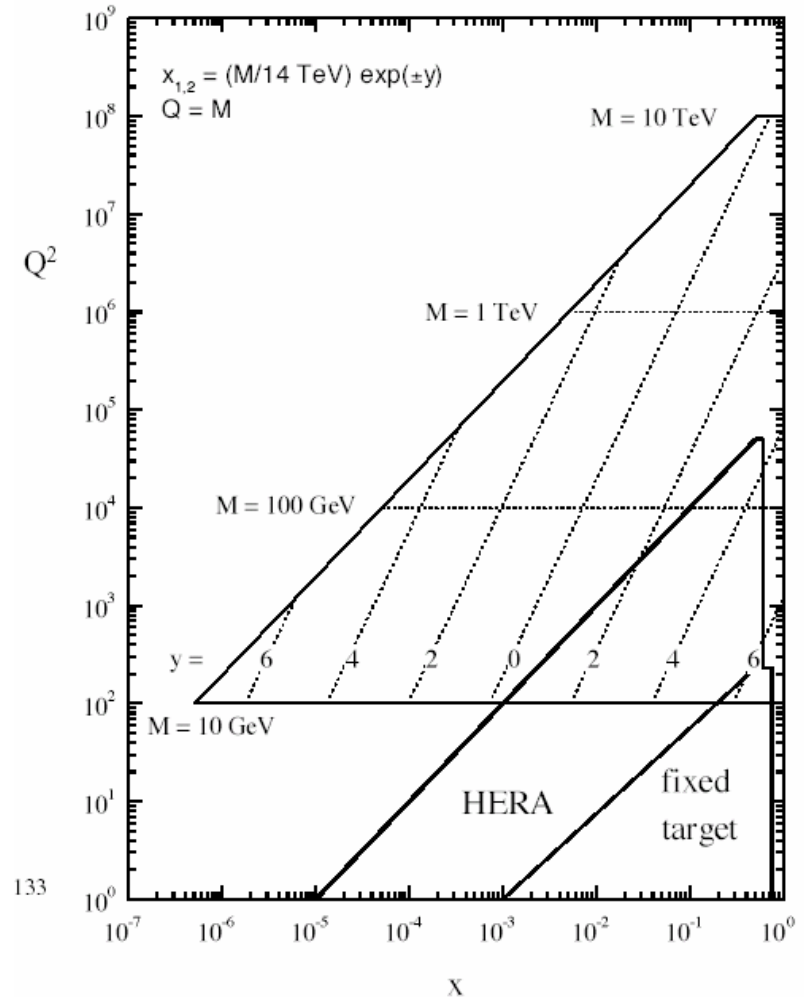
ZEUS



- Consistent with SM prediction
- Ratio of polarised cross sections, $\sigma^{e-p}(P=+29\%) / \sigma^{e-p}(P=-25.9\%)$
 - Precision statistically limited
 - Not yet conclusive observation of effect of longitudinal polarisation on cross sections.

Kinematic range including LHC

LHC parton kinematics



Shaper for FPC FEC

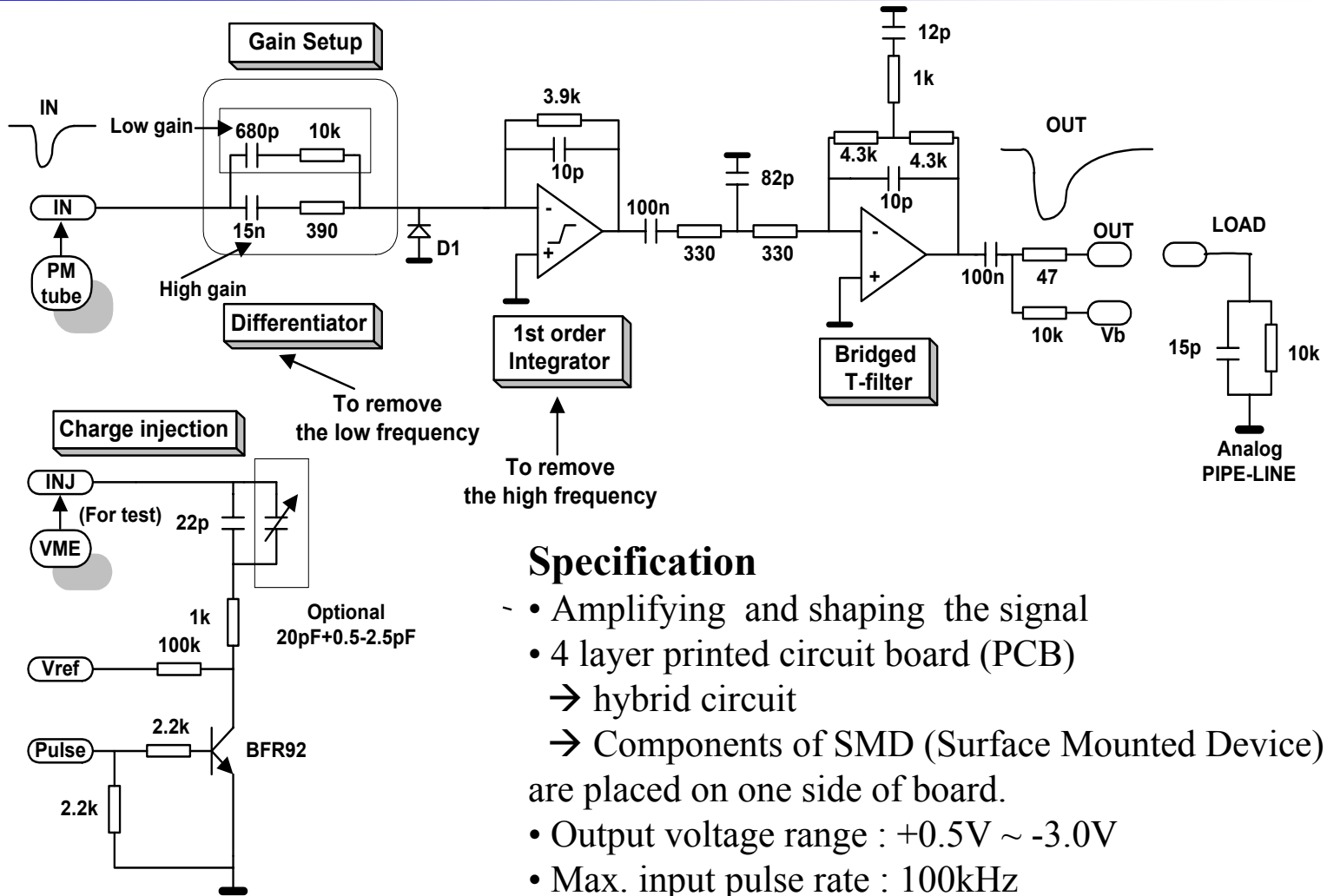
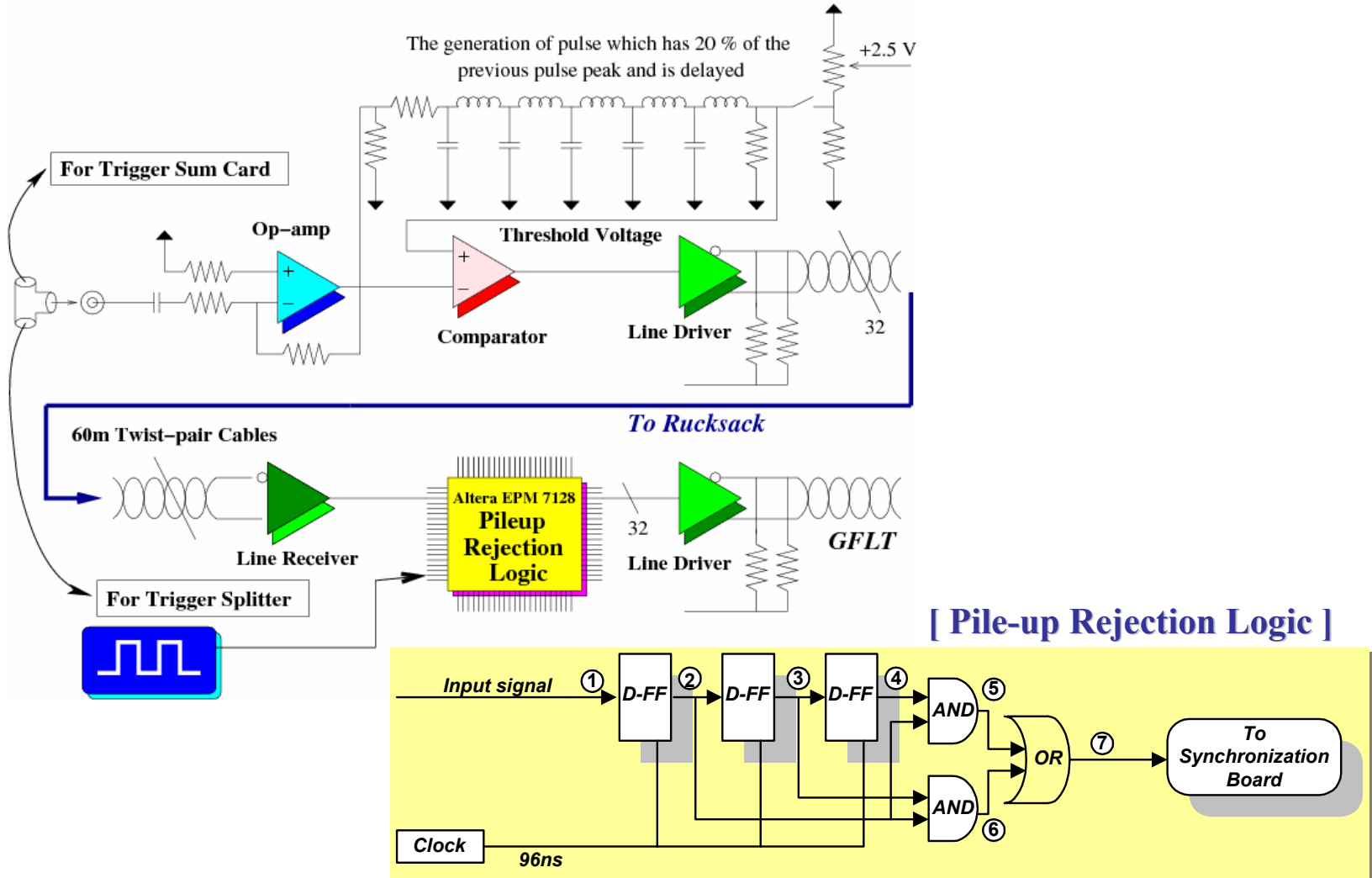
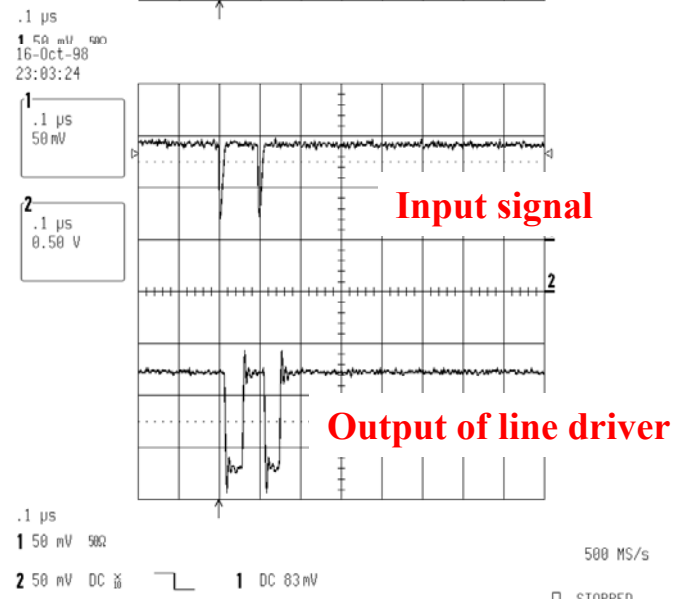
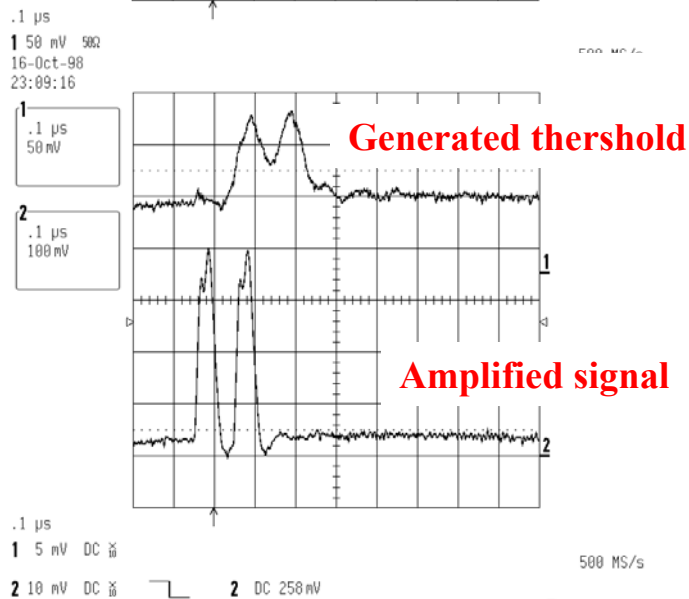
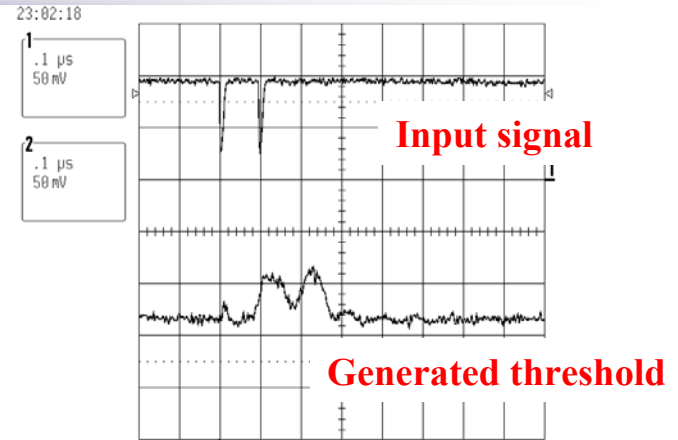
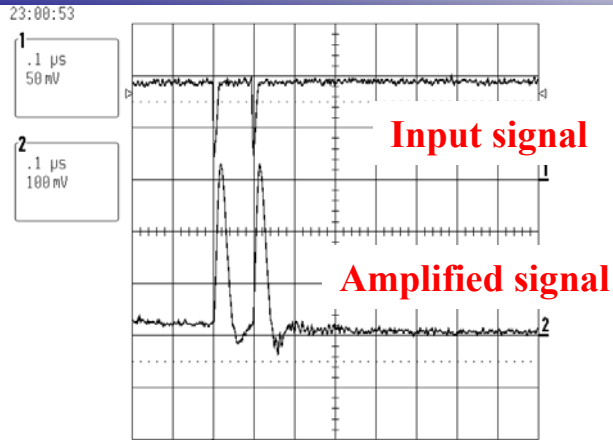


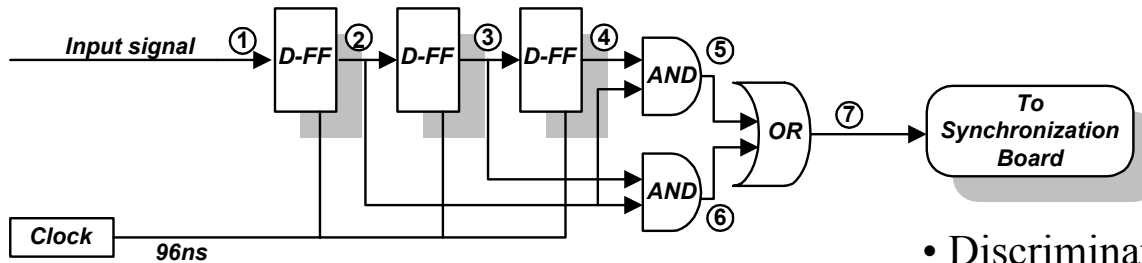
Diagram of Pile-up Rejection Card



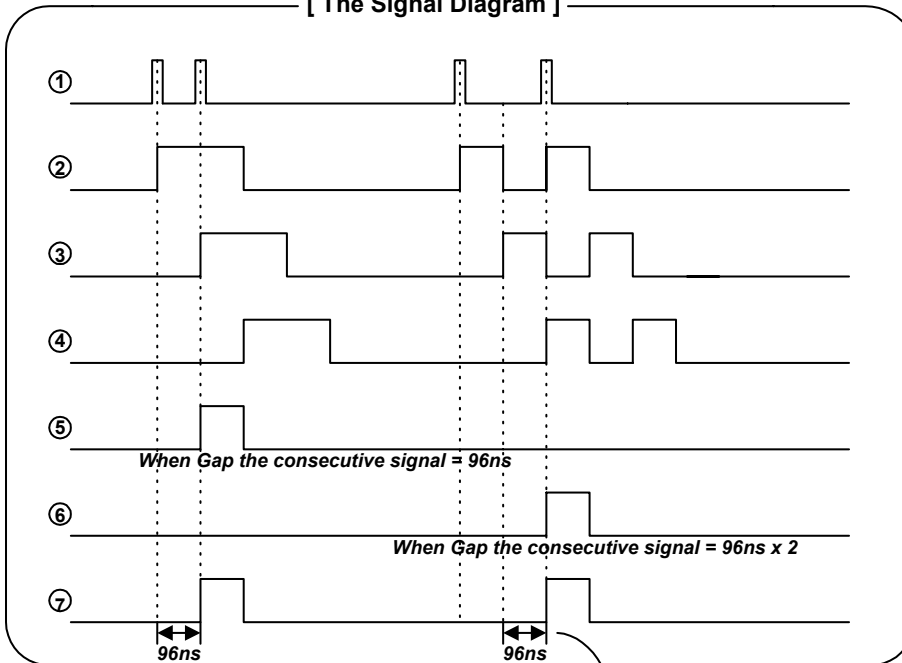
Signals from PRC as seen by an oscilloscope



PRC : Logic Card Design



[The Signal Diagram]



The Output which has pileup event,
is delayed as long as 96ns.

- Discrimination
the time gap : ONE or TWO clock
- Using *Altera EPM 7128*
- Procedure :
 - ① Input signal
 - ② After synchronized
 - ③ After one clock delay
 - ④ After two clock delay
 - ⑤ ② AND ③
to check the pile-up due to the incoming signal after one clock.
 - ⑥ ② AND ④
to check the pile-up due to the incoming signal after two clock.
 - ⑦ ⑤ OR ⑥ sending to GFLT.

Parton distribution from the ZEUS-S NLO QCD fit

Phys. Review D67, 012007(2003)

